Localization of infection in neonatal rhesus macaques after oral viral challenge

Roslyn A. Taylor[1], Michael D. McRaven[1], Ann M. Carias[1], Meegan R. Anderson[1], Edgar Matias[1], Mariluz Araínga[2], Edward J. Allen[1], Kenneth A. Rogers[2], Sandeep Gupta[3,4], Viraj Kulkarni[3], Samir Lakhashe[3,4] Ramon Lorenzo-Redondo[1,5], Yanique Thomas[1], Amanda Strickland[4], Francois J Villinger[2], Ruth M. Ruprecht[2,3,4], Thomas J. Hope[1*]

[1]Department of Cell and Developmental Biology, Northwestern University Feinberg School of Medicine, Chicago, Illinois, United States of America

[2]Department of Biology, New Iberia Research Center, University of Louisiana at Lafayette, Lafayette, Louisiana, United States of America

[3]Department of Microbiology, Immunology, and Molecular Genetics, University of Texas Health San Antonio, San Antonio, Texas, United States of America

[4]Disease Intervention and Prevention, Texas Biomedical Research Institute, San Antonio, Texas, United States of America

[5]Center for Pathogen Genomics and Microbial Evolution, Northwestern University Institute for Global Health, Chicago, Illinois, United States of America

*thope@northwestern.edu

Abstract

While vertical transmission of human immunodeficiency virus (HIV) can occur *in utero* and during delivery and through breastfeeding. We utilized Positron Emission Tomography (PET) imaging coupled with fluorescent microscopy of ^{64}Cu-labeled photoactivatable-GFP-HIV (PA-

GFP-BaL) to determine how HIV virions distribute and localize in neonatal rhesus macaques two and four hours after oral viral challenge. Our results show that by four hours after oral viral exposure, HIV virions localize to and penetrate the rectal mucosa. We also used a dual viral challenge with a non-replicative viral vector and a replication competent SHIV-1157ipd3N4 to examine viral transduction and dissemination at 96 hours. Our data show that while SHIV-1157ipd3N4 infection can be found in the oral cavity and upper gastrointestinal (GI) tract, the small and large intestine contained the largest number of infected cells. Moreover, we found that T cells were the biggest population of infected immune cells. Thus, thanks to these novel technologies, we are able to visualize and delineate of viral distribution and infection throughout the entire neonatal GI tract during acute viral infection.

Author Summary

Approximately 1.8 million children are currently living with human immunodeficiency virus (HIV). While mother-to-child HIV transmission can occur *in utero* and during delivery, it most commonly occurs through breastfeeding, creating the need to understand how the virus moves throughout the body and infects the infant once breast milk is consumed. Here, we used multiple imaging techniques and PCR to determine how HIV distributes throughout the gastrointestinal tract after oral viral exposure and in which tissues and cell types become acutely infected. We found that HIV rapidly spreads throughout and penetrates the entire gastrointestinal tract as early as four hours after exposure. We also found that the intestine contained the largest number of infected cells at 96 hours and that most cells infected were T cells. Our study shows that these imaging technologies allow for the examination of viral distribution and infection in a rhesus macaque model.

47

48 **Localization of infection in neonatal rhesus macaques after oral viral challenge**

49

50 **Introduction**

51 Mothers living with human immunodeficiency virus (HIV) and not on antiretroviral
52 therapy have up to a 40% chance of passing HIV to their children [1]. Despite findings that
53 suggest that exclusively breastfeeding infants can reduce HIV acquisition [2,3], breastfeeding
54 remains one of the main routes through which vertical HIV transmission occurs [1,4]. This most
55 likely occurs during the transition from breastfeeding to the introduction of solid foods [5] and
56 possibly through the premastication of food by people living with HIV [6]. Regardless of their
57 antiretroviral regimen, many women living with HIV need to breastfeed their infants due to
58 limited resources in developing countries where the overall benefit of breastfeeding outweighs
59 the risk for other life threatening infectious diseases, creating a great need to understand the
60 mechanism of mother-to-child HIV transmission through oral viral exposure.

61 Non-human primates (NHP) provide a model of and an opportunity to investigate oral
62 vertical HIV transmission *in vivo*. NHP models of oral HIV viral exposure results in rapid
63 systemic infection using various methods of viral delivery as it has previously been shown that
64 four-week-old neonatal rhesus macaques (RMs) have high viral blood titers after oral challenge
65 with SIVmac251, which inversely correlated to survival [7]. Likewise, additional studies have
66 proven similar; for example, direct application of SIVmac251 to tonsils and the check pouch
67 resulted in systemic viral infection within seven days and two weeks, respectively [8,9]. Another
68 study showed SIVmac251 DNA was concentrated in tissues of the head and neck, and systemic
69 viral dissemination occurred four days after exposure when delivered dropwise into the mouth

[10]. Lastly, recent reports also show that SIVmac251 RNA can be found in the brain and lungs 72 and 96 hours after challenge and SIV DNA is found throughout the gastrointestinal (GI) tract 96 hours after oral challenge [11].

HIV infects and depletes CD4+ cells in mucosal tissues, resulting in a decrease of CD4+ T cells in the blood [12,13]. CD4+ T cells in neonates have higher rates of cell metabolism, proliferation and "activated" cell phenotypes [14,15] making them prime candidates for viral infection. Therefore, the rapid spread of viral infection in infants is most likely due to this immature highly metabolic immune system [16,17]. To demonstrate this CD4+ T cell vulnerability to acute viral infection, Amedee et al., illustrated the presence of SIV RNA in tonsil and mesenteric lymph node T cells 72 hours after oral challenge [11]. Furthermore, another study reported that bottle fed neonatal RMs resulted in a reduction in CD4+ counts in the blood during systemic infection a week after viral challenge [18]. Furthermore, neonates have a higher number of CD4+ T cells in various tissues compared to adults [19,20], which could contribute to viral spread. In adult RMs, recent studies have focused on identifying which CD4+ T helper (Th) cell subsets are highly susceptible to HIV/SIV infection, with an emphasis on Th17 cells [21]. It has been shown that Th17 cells are preferentially infected in adult RMs after acute viral exposure in the female reproductive tract [22]. Additionally, Th17 cells have been shown to play an important role in HIV infection in the adult human colon [23,24]. The potential role of Th17 cells has not yet been elucidated in neonates.

Despite the advances in understanding mother-to-child transmission, the exact sites of viral distribution and entry in breastfed infants remains unknown. This study utilizes three different viruses (or virus-like particles) delivered in a bottle-fed neonatal RM model [25] to examine possible sites of viral entry and infection after acute oral viral exposure. First, whole

body Positron Emission Tomography and Computerized Tomography (PET/CT) imaging [26,27] was coupled with fluorescent microscopy of a photoactivatable-GFP HIV-BaL (PA-GFP-BaL) [28-30] to determine the distribution and localization of individual HIV virions two and four hours after viral challenge. Using PET/CT guided necropsy, we determined that HIV virions distribute to and penetrate the mucosal epithelium throughout the entire gastrointestinal (GI) tract, including the rectum, four hours after oral viral exposure. To study viral infection and viral cell targets, subsequent experiments used a dual viral challenge system, utilizing a non-replicative reporter virus [31] and a replicative SHIV-1157ipd3N4 [32]. Using our non-replicative reporter virus, we found the tongue may be a main site of viral transduction. Additionally, in congruence with previous findings [9-11], we found that the entire GI tract is susceptible to SHIV-1157ipd3N4 infection 96 hours after oral challenge. Likewise, the small intestine was identified as the tissue that held the biggest foci of infection by fluorescent deconvolution microscopy, with T cells encompassing the largest infected population of cells. These findings can provide mechanistic insight and increase our understanding of mother-to-child transmission after viral exposure.

Results

PET/CT imaging illustrates that HIV virions distribute throughout the GI tract four hours after oral viral exposure

The technologies of PET/CT imaging, photoactivatable HIV (PA-GFP-BaL), and fluorescent deconvolution microscopy [28-30] were combined to determine where virus distributes throughout the body after oral exposure. PET/CT imaging allows for the *in vivo* tracking of virions over time after challenge through radiolabeling PA-GFP-BaL with a

radioactive isotope of copper, ^{64}Cu (**Fig 1A**). During tissue processing, tissues are cut into 1cm pieces, frozen into blocks with optimal cutting temperature medium (OCT), and each block is scanned to identify individual blocks with positive radioactivity, thereby increasing our chances of finding HIV virions by microscopy (**Fig 1B and 1C** [30]). These experiments occurred in pairs, with one two-hour animal and one four-hour animal for each experimental day. The same viral stock was used in all four animals.

Two hours after oral exposure of PA-GFP-BaL-^{64}Cu, PET scans revealed radioactivity throughout the GI tract up to the transverse colon in both two-hour animals. Four hours after oral exposure, radioactivity was observed throughout the GI tract to the colon including the length of the rectum (**Fig 2A-D**). In one of the four-hour animals, PET signal was not found past the descending colon, which was most likely due to a bubble of trapped gas that was observed upon colon resection (**Fig 2C**). PET imaging of individual tissue blocks confirmed our findings from the whole-body PET imaging in all four animals (**Fig 1B**); despite the gas obstruction observed in one animal, individual radioactive blocks up to and including the transverse colon were found in both two-hour animals and throughout the length of the GI to the rectum in both four-hour animals **(Fig 2C).**

HIV virions distribute throughout the entire length of the GI tract four hours after oral viral exposure

Next, fluorescent deconvolution microscopy was performed to identify the total number of individual HIV virions (non-penetrating and penetrating) in individual tissue blocks that had strong radioactivity by PET imaging (**Fig 1C**). Penetrating virions were defined as being one micron from the epithelial surface. Because virions were not found in every tissue of the GI tract

in all animals, the GI tract was dichotomized into upper (esophagus and stomach) and lower (small intestine and colon) sections. Although the distance to which HIV virions distributed after oral challenge extended to the transverse colon, the majority of the virions were located in the oral cavity (buccal, tongue, and tonsil; mean = 26.5 virions, frequency = 0.97) in animals necropsied two hours post-challenge. We also observed significantly fewer numbers (FDR<0.05) and a lower frequency of virions both in the upper (mean = 1.67 virions, frequency = 0.50) and lower (mean = 2.25 virions, frequency = 0.22) GI tract compared to the oral cavity two hours after viral exposure (**Fig 2E, F**). However, in the four-hour animals, fewer virions were found in the oral cavity (mean = 0.75 virions, frequency = 0.03). The highest number of the virions found in the four-hour animals was in the lower GI tract (mean = 7.83 virions, frequency = 0.78; **Fig 2E, F**). The same number and frequency of virions were found in the upper GI tract (mean=1.67 virions, frequency = 0.50) in the four-hour animals as the two-hour animals.

Similar results were found when specifically examining the number of virions that penetrated into the mucosa (**Fig 2G**). In the two-hour animals, the largest number of penetrating virions were found in the oral cavity (sum of virions in both two-hour animals: non-penetrating = 26 virions, penetrating = 80 virions) with statistically significant differences observed both between this cavity and the upper (non-penetrating = 3, penetrating = 7) and lower GT tract (non-penetrating = 9, penetrating = 15; FDR<0.05). Likewise, in the four-hour animals, the majority of penetrating virions were found in the lower GI tract (non-penetrating = 19 virions, penetrating = 75 virions), although among the very few virions found in the oral cavity, all of them were penetrating virions (penetrating = 3). In the upper GI tract, few virions were found at four fours (non-penetrating = 1, penetrating = 8) There was no difference in penetration depth between location of virion or time point after oral challenge (**Fig 2H**) with the exception of the

few virions found in the oral cavity at four hours that proportionally were also significantly deeper penetrators. These data, combined, demonstrate the validity of PET/CT to identify areas of virus accumulation along with illustrating that HIV virions can distribute throughout the entire GI tract four hours after oral viral exposure in neonates.

Validating our dual challenge oral transmission model

While PET/CT and PA-GFP-BaL-^{64}Cu experiments allow for the visualization of virion distribution and penetration into mucosal tissues, these technologies do not allow for the examination of viral infection. Therefore, to study viral infection, subsequent experiments orally challenged neonatal RM with LICh, a non-replicative reporter virus [31], and a replicative SHIV-1157ipd3N4 [32]. Our lab has previously shown that we can locate and identify cells that were first transduced by the challenge inoculum through a viral vector, LICh [31]. Due to the lack of accessory genes in LICh, the replication process gets halted after one round of viral integration, thus resulting in viral transduction. In a proof-of-principle experiment, one animal was orally challenged with 8mL of LICh alone and then sacrificed at 96 hours after challenge to validate whether LICh can be used to identify sites of viral transduction after oral challenge. Tissues from the GI tract were extracted and analyzed by IVIS. We were able to identify luciferase signal on IVIS in the esophagus, neck lymph nodes, and stomach of neonatal RMs at 96 hours after oral exposure (**Fig 3A**).

Identifying tissues susceptible to viral transduction and infection

Since we were able to observe luminescence by IVIS after oral challenge, we proceeded to use a dual viral challenge model for the remaining experiments. We have previously shown

that LICh can be used as a guide to locate areas of replicative foci of infection, as LICh disseminates throughout the body similar to replicative viruses [22,31]. Because LICh does not replicate, an SIV containing an R5-tropic HIV Clade C *env* genes, SHIV-1157ipd3N4, was used to study viral replication. Because LICh does not contain accessory genes, we could distinguish SHIV-1157ipd3N4 infected cells from LICh transduced cells by examining replicative viral infection by gag DNA and protein. To identify tissues that are initially susceptible to viral transduction and infection, genomic DNA was extracted and performed nested PCR to target mCherry and gag DNA. In a proof-of-principle experiment, one neonatal RM (RM13) was challenged with four feedings of 2mL of LICh and a repeated low dose of SHIV-1157ipd3N4 (see Experimental Methods) and necropsied shortly after two days of viral challenge to examine early transmission events. Results from the low dose challenge and 53-hour time point showed less transduction and infection, as predicted. At 53 hours post-oral challenge, we found mCherry DNA in the top of the tongue **(Table 1)**. Gag DNA was found in the neck lymph nodes, stomach, and small intestine at 53 hours post-challenge.

Table 1: Distribution of LICH transduction and SHIV-1157ipd3N4 DNA throughout the GI tract after oral challenge

Animal	Challenge	Tongue	Cheek	Soft Palate	Tonsil	Neck Lymph Nodes	Esophagus	Stomach	Small Intestine	Large Intestine	Spleen	Liver
RM13	Low Dose 53 hrs	+				#	#	#	#			
RM10	High Dose 96 hrs	+	#	#	#		#	+	+#	#	#	#
RM17	High Dose 96 hrs	+#	#		#	#	#	#	#	#	#	

LICh viral vector mainly found in the tongue after oral challenge. SHIV-1157ipd3N4 viral dissemination found throughout the GI tract after oral challenge. + indicates mCherry DNA found; # indicates gag DNA found

For the next set of experiments, eight neonatal RMs were orally challenged with a repeated high dose challenge of SHIV-1157ipd3N4 and one 8mL bolus of LICh, which was given during the last bottle feeding, and the time between challenge and necropsy was extended to 96 hours prior to nested PCR and fluorescent microscopy being performed, increasing the potential of finding infected cells and of understanding the mechanism of viral transduction and infection in our bottle-feeding model. While luciferase activity was previously observed in the proof-of-principle study, when this group of eight neonates were examined by IVIS, very little luciferase activity was seen among all the animals; therefore, we performed nested PCR on all processed tissues. Nested PCR revealed mCherry DNA in the tongue, stomach, and small intestine in RM10 and in the tongue of RM17. At 96 hours, SHIV-1157ipd3N4 viral dissemination was more widespread. Gag DNA was found in the cheek, tonsil, soft palate, esophagus, mesentery, small intestine, large intestine, liver, and spleen of RM10. Gag DNA was also in the cheek, tongue, tonsil, the transformation zone to the stomach from the esophagus, small intestine, large intestine, spleen, and neck lymph nodes of RM17 **(Table 1)**. When performing nested PCR, large amounts of tissues are sectioned for DNA isolation. Therefore, to minimize tissue sample depletion, future experiments primarily focused on fluorescent microscopy to identify viral transduction instead of utilizing nested PCR to identify infected tissues.

LICh transduction identifies initial target cells after oral viral challenge

Tissue sections were then examined by fluorescent deconvolution microscopy to identify individual LICh transduced cells at 96 hours **(Table 2, Fig. 3)**. After a careful and thorough examination of all tissues, an $mCherry^+$ cell was found in the tongue of RM22 **(Fig. 3B)**.

Spectral imaging confirmed that the emission spectrum on this cell matched the known emission peak of mCherry, 610nm, **(Fig. 3C)**, confirming that this cell in the tongue of RM22 was LICh transduced from the challenge inoculum. Additionally, the trachea of RM23 also contained an mCherry$^+$ cell and the stomach of RM25 had several mCherry$^+$ cells. All the cells were validated as mCherry$^+$ on spectral imaging **(Table 2)**. However, although we were able to detect and verify mCherry+ cells in a few animals, these cells proved difficult to widely identify due to the high autofluorescent background in the neonatal tissues. Therefore, tissue sections that contained luciferase activity by IVIS were also stained with antibodies for luciferase. Unfortunately, despite tissues showing luciferase activity by IVIS, positive luciferase signal was not detected in any of the neonatal tissues **(Fig. 3D)**. Although, we previously used a LICh viral vector in a model of SIV infection in the female reproductive tract to identify sites of viral transduction [31], these data suggest that in our oral viral challenge model, LICh technology may not be as efficient. Therefore, defining SHIV-1157ipd3N4 viral infection, replication, and dissemination in the oral and gut mucosa was prioritized.

Table 2: Localization of LICh transducedcells at 96 hours post oral challenge by microscopy

Animal	Tongue	Tonsil	Stomach
RM10			
RM17			
RM22	+		
RM23		+	
RM25			+
RM26			
RM27			
RM28			

LICh transduced cells found in the tongue, trachea, and stomach 96 hours after oral challenge by microscopy. Cells

were validatedby spectral imaging. + indicates mCherry DNA found

Most infected cells are found in the small intestine after oral viral challenge

To determine which cell types are susceptible to replicative viral infection after oral exposure, tissues were examined for evidence of SHIV-1157ipd3N4 infection using fluorescent deconvolution microscopy (**Table 3**). Tissue sections from the oral cavity and GI tracts of each animal were stained with antibodies directed toward SIV Gag (clone AG3) to identify SHIV-1157ipd3N4 gag, as well as CD3 and CCR6 to phenotype infected immune cell subsets **(Fig. 4, Table 3)**. Five panels consisting of three 40x by five 40x images were taken for phenotype analysis. As we have previously shown, these markers allow us to identify the target cells as Th17, T cells, immature dendritic cells (iDCs), and other. In the tongues of neonatal RMs, we found very small foci of infection; five of the eight animals examined had SHIV-1157ipd3N4 infected cells (5.86 ± 7.36 cells, median = 4**, Fig. 4C)**. Similar to what was observed in the tongue, the tonsils contained a small number of SHIV-1157ipd3N4 infected cells in six of the animals (13.5 ± 19.93 cells, median = 4), corroborating previous studies illustrating tonsils as a site of potential viral entry after oral viral challenge [8,10,18,33]. The fewest number of infected SHIV-1157ipd3N4 cells in terms of number of animals and quantity of cells were in the esophagus (5 ± 12.55 cells, median = 0.5). While SHIV-1157ipd3N4 infected cells were detected in the tongue, tonsils, and esophagus, it was not a common event. In contrast, the stomach contained larger foci of infection compared to those found in the oral cavity and esophagus; all eight RMs had infected cells in the stomach (43.63 ± 60.82 cells, median = 20).

Table 3: Localization of SHIV-1157ipd3N4 infected cells 96 hours after oral challenge by microscopy

Animal	Tongue	Tonsil	Esophagus	Stomach	Small Intestine	Large Intestine	Mesenteric Lymph Nodes
RM10	+	+	+	+	+	+	
RM17		+		+	+	+	NA
RM22		+		+	+	+	+
RM23	+	+	+	+	+	+	+
RM25	+			+	+	+	NA
RM26	+	+	+	+	+	+	NA
RM27	+	+	+	+	+	+	NA
RM28				+	+	+	NA

SHIV-1157ipd3N4 viral dissemination found throughout the GI tract after oral challenge. + indicates AG3+ cells found by microscopy, NA indicates mesenteric lymph nodes were not collected from this animal

Previously, it has been shown that the intestines are a site of viral expansion in neonates after intravenous infection [34]; therefore, we examined the small intestine, large intestine, and their draining mesenteric lymph nodes for foci of SHIV-1157ipd3N4 infection to see if we could identify similar after oral challenge. All eight RMs in the study had SHIV-1157ipd3N4 infected cells throughout the small and large intestine. The small intestine contained the largest foci of infection in all eight neonates (367.1 ± 250.8 cells, median = 308, **Fig. 4A-B).** Overall, the large intestine had the second largest foci of infection in the neonates (159.4 ± 88.39, median = 176.5, infected cells, **Fig 4.C, Fig. 5A).** Unfortunately, we were only able to obtain the mesenteric lymph nodes from three of the eight animals; however, we found SHIV-1157ipd3N4 infected cells in the mesenteric lymph nodes of two of these three animals (**Table 3**). These data suggest that viral replication can be found throughout the GI tract, all the way to the distal large intestines and the corresponding mesenteric lymph nodes after oral viral challenge.

The majority of SHIV-1157ipd3N4 infected cells throughout the gut are T cells at 96 hours after oral viral challenge

It has previously been shown that neonates have CD4+ T cells of a memory phenotype that proliferate at high rates in mucosal tissues, which may make these T cells the primary target of HIV/SIV infection [34]. Immature dendritic cells (DC) have been suggested to be initial targets and mediators of HIV/SIV [35-37] infection. Our lab has previously shown that Th17 cells are preferentially infected after vaginal SIV challenge [22]. Taking all these results together, we stained our tissue sections for T cell marker CD3 and the chemokine receptor CCR6 to investigate which cell types are infected after oral challenge. Infected cells were phenotyped into the following groups: Th17 T cells (CD3+ CCR6+ AG3+), other T cells (CD3+ AG3+), Immature DC (CCR6+ AG3+), and other (AG3+). Due to the small number of SHIV-1157ipd3N4 infected cells found in the tongue, tonsil, and esophagus, our phenotyping analysis focused on the stomach, small intestine, and large intestine. In the stomach, the majority of infected cells were other T cell subsets when examining all eight neonates combined **(**n= 242 cells, 68.95%, **Fig. 5B)**. Overall, Th17 T cells were the second largest infected population in the stomach (n=78 cells, 22.22%). Individually, Th17 T cells made up the largest group of infected cells in three of the RMs (RM17, RM22, RM26), while other T cell subsets were the largest group of infected cells in 4 of the RMs **(**RM23, RM25, RM27, RM28, **SFig 1)**. Other cell types made up 6.55% of total infected cells (n=23 cells) and immature DC were 2.28% of infected cells (n=8 cells) in the stomach. One neonate, RM10, had very few infected cells (n=3), however 33.33% of infected cells of Th17 cells, (n=1 cell) other T cells subsets (n=1 cell), and immature DC (n=1 cell, **SFig 1**). The largest infected population of cells in the small intestine was other T cells in all eight neonates **(**n=2468 cells, 76.74%, **Fig 5B, SFig 1)**. The second

largest infected population found in the small intestine was Th17 T cells (n=655 cells, 20.37%). Similar to the stomach, few other cell types (n=86 cells, 2.67%) and immature DC (n=7 cells, 0.22%) were infected in the small intestine. Other T cell subsets were marginally infected with the most in the large intestine (n=651 cells, 51.06%). For example, the large intestine was the site of the greatest infection in Th17 T cells (n=608 cells, 47.69%, **Fig 5B, SFig 1**); the majority of infected cells in half of the neonates were Th17 T cells (RM10, RM17, RM26, RM27), while other T cell subsets were in the remaining four (RM22, RM23, RM25, RM28). Very few infected immature DC (n=10 cells, 0.78%) and other cell types (n=6 cells, 0.47%) were found in the large intestine. Overall, our data suggest that T cell subsets that are not Th17 are the greatest target of infection in our oral transition model, unlike our previous findings after vaginal challenge [22]. Among all of the animals and tissue types analyzed, very few immature DC and other cell types were infected.

Discussion

Previous studies using intravenous inoculation of infant rhesus macaques have provided great insights into the susceptibility of neonatal RMs to SIV infection [38,39] and CD4+ depletion in the gut after challenge [14,15,34]. However, breastfeeding remains the most prevalent route for vertical HIV transmission worldwide [1]. This creates a great need to study oral transmission in neonatal animal models. Here we show that, in a bottle-fed model, HIV virions rapidly distribute throughout the GI tract and intact particles found as far as the rectum four hours after oral exposure (**Figs 1 and 2)**. We also show that the greatest number of SHIV-1157ipd3N4 infected cells is in the small intestine and that T cells are primarily infected 96 hours after viral exposure (**Figs 4 and 5**).

To determine how HIV virions distribute throughout the body immediately after oral exposure, we radiolabeled a photoactivatable, fluorescently tagged HIV and performed *in vivo* PET imaging coupled with deconvolution fluorescent microscopy (**Figs 1 and 2)**. While these PET/CT experiments are not studying viral infection, these technologies provide insight into how HIV disseminates throughout the body, and where in the oral mucosa and GI tract the virus enters the mucosa after oral viral exposure. We found that two hours after oral challenge, HIV virions mainly localize in the oral cavity, but then further disseminate to the transverse colon. Four hours after challenge, HIV virions are found throughout the small and large intestine; in both four-hour animals, many virions were also found within the rectum. These experiments revealed that HIV distributes throughout the GI tract rapidly after oral challenge. In a matter of two hours, the majority of total virions and penetrating virions changed from the oral cavity to the lower GI tract consistent with virion penetration of epithelial barriers happening in a wave followed by lysis or turnover because the signal was lost at the two-hour timepoint (**Fig 2)**. It has been reported that the gastric juice of neonates has a relatively neutral pH compared to adults, ranging mostly between 7.5 and 8.5, which could explain how the virus was able to survive and pass through the stomach of the neonatal RMs [40].

Previously, it has been suggested that the tonsils may be a portal of viral access to susceptible immune cells after oral exposure [8,10]; however, these studies directly applied virus to the tonsils. We found very few SHIV-1157ipd3N4 infected cells in these tissues 96 hours in our bottle-fed model of oral viral exposure (**Figs 4C and 5A)**. Although these data do not discount the tonsils as a potential source of initial viral entry, it suggests that this area may not be the primary or major portal of entry for initial infection and viral dissemination. It is notable that the tonsils are more similar to lymph nodes than the mucosal environment of the small and large

intestine. Importantly, most of the T cells in the tonsil do not express the mucosal homing receptor CCR5, which is a required co-receptor which in combination with CD4 is required for the virion to functionally fuse with the target cell membrane. The paucity of susceptible T cells (CCR5+) in the tonsils is the likely reason that we found limited numbers of SHIV-1157ipd3N4 infected cells in the tonsil and oral cavity overall. In contrast, the gut contains a large number of potential SHIV-1157ipd3N4 target cells with CCR5+, CD4+ T cells being the majority population in the immune cell rich mucosal environment of the intestine. This makes the gut a rich environment for the virus to replicate which is reflected in the presented data, especially the small intestine (**Figs 4 and 5).** Considering our observations, our data suggests that the gut may represent the major portal of viral transmission after oral exposure by breastfeeding. Consistent with this possibility, the distribution of viral particles in a liquid, oral challenge rapidly reaches the stomach and intestines where there will be ample opportunity for the virus to reach and penetrate the luminal barrier of the gut. In contrast, the fluid in the inoculum will rapidly flow over the surface of the oral cavity giving less of an opportunity to penetrate the epithelial barriers of the oral cavity which is target cell poor environment. While we found the majority of SHIV-1157ipd3N4 cells in the small and large intestine, it is important to note that we cannot determine with our methods if these large foci of infection represent the initial sites of infection at the portal of transmission or a location rich in target cells that can foster high levels of viral replication after initial expansion and replication in the oral cavity. It seems the large number of expanding, substantial infectious foci in the gut most likely initiated in the gut considering the short four-day period between drinking virus containing fluid and necropsy. The efficient movement of the virus containing fluid we documented throughout the alimentary canal four hours after drinking and our ability to identify intact viral particles penetrating the intestinal

mucosa likewise support a model where oral exposure of virus containing fluid can utilize the intestine as a portal of transmission.

Another retrovirus known to be milk transmitted is the mouse mammary tumor virus (MMTV) that disseminates through the GI tract and directly infects immune cells in the Peyer's patches of the gut, suggesting that other breast milk-transmitted retroviruses may also have this capability [41,42]. Although current models of MMTV acquisition suggest that this process takes place through cell-associated virus (infected cells in milk) which could withstand the acidic pH of stomach acid better than cell-free virus [43]. However, our observations clearly demonstrate the viral particle can reach the intestinal compartment intact, without being cell associated, agreeing with previous results from Baba et. al. which demonstrated that cell-free SIV is transmitted orally in neonatal rhesus macaques [38]. Providing the challenge virus in formula may have played a role in buffering the mucosal environment slowing virion lysis and degradation. Therefore, our PET/CT and microscopy data, taken together with the knowledge that the gut is a target rich environment for viral infection is consistent with a model where the SHIV-1157ipd3N4 infected cells we found in the intestines originated from virus in the challenge inoculum utilizing the gut as the primary portal of transmission. Future experiments are required to determine the origin of the foci of infection we observed.

Our lab has previously shown that the reporter viral vector, LICh, allows us to locate tissues and cells that were transduced by the challenge inoculum through bioluminescence, nested PCR and fluorescent microscopy [22,31]. This technology provides us with the ability to identify cell types that are vulnerable to becoming the first cell infected in different models of HIV transmission. In our model of oral HIV transmission, we were able to use LICh to identify sites of viral transduction through the presence of mCherry DNA by PCR (**Table 1)**. However,

393 locating mCherry+ cells by microscopy was arduous (**Fig 3 and Table 2)**. It may be possible
394 that, while our viral vector works well in rectal and vaginal infection models, this technology is
395 not well suited for oral challenge. Visualizing LICh is optimal with a focal area of transduction
396 to produce a sufficient density of photons for efficient detection. Therefore, a target poor
397 environment like the tonsils may not be able to achieve sufficient photon flux for detection.
398 Likewise, the particles will be greatly diluted and at low concentration to transduce cells at a
399 density conducive to the detection of luciferase activity. Because of inefficient photons to guide
400 our efforts to identify pieces of tissue containing foci of transduction, we decided to forgo
401 searching for LICh transduction in subsequent animals (RM23, RM25, RM26, RM27, RM28)
402 and proceed to identify SHIV-1157ipd3N4 infected cells. The large replicative capacity of the
403 virus, and infectious clone engineered to contain NF-κB sites in the long terminal repeats [32],
404 facilitated our ability to identify pieces of tissue containing foci of viral replication random
405 screening.
406 Models of mother-to-child transmission that have used oral routes of inoculation utilized
407 either dripping virus directly onto the tonsils [9,10,18,44], slowly dripping cell-free virus
408 solution onto the back of the tongue [38] or bottle-feeding methods [18,45]. To mimic how
409 vertical transmission occurs in humans via breastfeeding, we mixed challenge inoculums into
410 formula, which was then bottle fed [25]. Currently, the exact dose of HIV in each exposure
411 during breastfeeding in humans is unknown [1]. It has been shown that human breast milk viral
412 load can range widely from a hundred copies per milliliter to millions of copies per milliliter.
413 These studies have also shown that a high viral load in breast milk correlates to HIV
414 transmission in human infants [46-48]. Our initial experiments were based on repeated low dose
415 viral challenges as other studies have previously reported [18,44]. We found SHIV-1157ipd3N4

DNA (**Table 1)**, however, viral dissemination was not as widespread as we predicted using the repeated low challenge dosing. Therefore, to better understand the mechanisms of viral dissemination after oral challenge, we increased the dose of virus in our repeated challenges to super-physiological. From these changes in experimental design, along with an increase in time point to day four post viral challenge, infected cells could be detected easily throughout the GI tract (**Figs 4, 5, and S1 and Table 3)**.

Neonates have an immature innate and adaptive immune system that is highly metabolically active compared to adults [17], providing an optimal environment for viral replication which often results in a high viremia. We have previously observed that immature DCs are efficient targets of SIV infection after vaginal challenge [22,31]. They can also play roles in HIV/SIV transmission in other models [35-37]. However, immature DCs are not a preferential target of the SHIV-1157ipd3N4 virus utilized in this neonatal model of oral viral exposure. For example, it has previously been shown that neonates have more proliferating CD4+ T cells in the small intestine than adult macaques and that these proliferating T cells are selectively infected after intravenous injection of SIVmac251 in neonates [14,15]. Similarly, our data show that T cells, specifically non-Th17 T cells, were the largest subset of infected immune cells in all tissue types analyzed after oral SHIV-1157ipd3N4 challenge (**Figs 5 and S1**). However, it is important to note that we did not look further into what CD4+ T cell subset makes up our "other T cell" population. This remains to be investigated in future experiments.

These data demonstrate that HIV virions distribute throughout and penetrate the entire GI tract at a very rapid rate hours after viral exposure. These findings were only made through use of our technologies of PET/CT coupled with a photoactivatable GFP-tagged HIV. Furthermore, we also show that the entire GI tract is susceptible to viral infection after oral viral exposure. Our

data indicate that the small intestine is the primary site for viral infection and that CD4+ T cells are the primary target cells 96 hours after viral exposure. Taken together, our results provide more insight to the mechanism behind acute viral infection in neonates after oral exposure.

Experimental Methods

Ethics Statement

PET/CT experiments were conducted at the New Iberia Research Center (NIRC) at the University of Louisiana at Lafayette. Studies examining LICh transduction and SHIV-1157ipd3N4 infection were conducted at the Southwest National Primate Research Center at the Texas Biomedical Research Institute (Texas Biomed), in San Antonio, Texas All procedures were approved by the Animal Care and Use Committees at Texas Biomed (IACUC: 1441 MM) and NIRC (IACUC: 2017-8791-002). All studies were performed in accordance with the recommendations in the Guide for the Care and Use of Laboratory Animals.

Virus production

To generate PA-GFP-BaL, we co-transfected the R5-tropic, R9-BaL infectious molecular clone construct with a plasmid expressing a photoactivatable GFP (PA-GFP) [49] fusion with HIV VPR (PA-GFP-VPR) as previously described [28-30]. The replication competent virus labeled with PA-GFP-VPR generated by polyethylenimine transfection of human 293T cells in DMEM medium containing 10% heat-inactivated fetal calf serum, 100U/ml penicillin, 100µg/ml streptomycin, and 2mM l-glutamine. After 24 to 48 hours, virus was harvested, filtered at 0.45 µm and stored at -80°C [28]. Viral particles were concentrated and enriched by centrifugation through a sucrose cushion.

LICh reporter virus was produced as previously described [31]. Briefly, a SIV-based pseudovirus vector system was generated from modifications of the SIV3 vector system [50]. The firefly luciferase gene is expressed through a poliovirus internal ribosome entry site (IRES) [51]. Transcription of both luciferase and mCherry are driven from the constitutive immediate-early CMV promoter and their expression is enhanced by WPRE for robust expression. LICh is produced by transfecting 293T cells with four plasmids: LICh reporter genome, SIV3+ packaging vector, REV expression plasmid DM121, and JRFL envelope. Viral supernatants were collected 48 hours post-transfection, purified through 0.45μm filters, concentrated over sucrose cushions, and resuspended in PBS. Concentrated virus was stored at −80°C.

SHIV-1157ipd3N4 was generated as previously described [32]. Naïve RM peripheral blood mononuclear cells (PBMCs) were stimulated with concanavalin-A, followed by infection with SHIV-1157ipd3N4 that was harvested from 293T cells in the presence of human IL-2 (20U/mL) and TNF-α (10ng/mL). The PBMC-derived virus stock has a p27 concentration of 227ng/mL and $4x10^6$ $TCID_{50}$ per mL as titrated in TZM-bl cells.

DOTA-labeling of virus

HIV virus was DOTA-labeled as previously described [26,30]. PA-GFP-BaL was labeled with a dodecane tetraacetic acid (DOTA) chelator, which allowed for attachment of ^{64}Cu. Two buffers were prepared using a chelating resin to remove all free copper: 0.1 M sodium phosphate buffer (pH 7.3) and 0.1 M ammonium acetate buffer (pH 5.5). Chelex 100 Chelating Resin (5g, BioRad, Hercules, California) was added to 100 ml of each buffer, incubated with stirring for 1 hour at room temperature, and filtered at 0.22 μm for sterilization. Concentrated virus was resuspended in PBS and a 1:10 volume of 1 M sodium bicarbonate added. DOTA-NHS-ester (Macrocyclics, Dallas, Texas) was dissolved in the 0.1 M sodium phosphate buffer. The two

484 solutions were combined (0.3mg DOTA-NHS-ester per 500ng of virus, as detected by p24
485 assay), and incubated on a rocker in the dark at room temperature. After 30 minutes, the buffer
486 was exchanged for the 0.1 M ammonium acetate using a Zeba column 40K (Thermo Fisher
487 Scientific, Waltham, Massachusetts), wash steps completed per manufacturer's protocol, and
488 virus (PA-GFP-BaL-^{64}Cu) collected and frozen for shipment to New Iberia Research Center
489 (NIRC) at the University of Louisiana at Lafayette.

490 **^{64}Cu labeling of virus particles**.

491 A solution of $^{64}CuCl_2$ (University of Wisconsin-Madison) was neutralized with Chelex-
492 treated 1 M NH_4OAc (Sigma) to a pH of 5.5, and an aliquot (~185MBq) incubated with DOTA-
493 PA-GFP-BaL stock at 37ºC for one hour. The sample was purified with a Zeba desalting spin
494 column (30K MWCO, Thermo Fisher), eluted with PBS (Thermo Fisher), and labeling
495 efficiency was evaluated. Labeled virus (10–37MBq) was mixed with unlabeled virus
496 immediately prior to oral challenge.

497 **Non-human Primate Studies: oral viral challenge**

498 In total, 14 Indian-origin rhesus macaques (*Macaca* mulatta) were used. Four animals
499 that were used for PET/CT experiments received 2mL of PA-GFP-BaL (1,000ng/mL) + 0.25mL
500 of PA-GFP-BaL-^{64}Cu ((1,000ng/mL) in 2mL of Pedialyte for a total volume of a 4.25mL feeding
501 (25). One animal was inoculated with a single dose (8mL) of LICh reporter virus and sacrificed
502 at 96 hours to generate proof-of-principle data (**Fig. 3**). One animal was inoculated with four
503 doses of 2mL of LICh + 3.5mL SHIV-1157ipd3N4 (8mL of LICh and 14mL of SHIV-
504 1157ipd3N4 in total) and sacrificed at 53 hours for a low dose, early time point challenge (**Table**
505 **1**). The remaining eight animals were challenged via eight feedings of 5mL SHIV-1157ipd3N4
506 (for a total of 40mL of SHIV115ipd3N4 over the course of the experiment) + one dose of 8mL

LICh, which was included in the final feeding (**Supplemental Table 1).** All animals were inoculated with virus that was mixed with Pedialyte via oral bottle feeding. Animals were humanely sacrificed with an overdose (100mg/kg) of pentobarbital while under isoflurane anesthesia (Euthasol, Virbac, Westlake, Texas) or telazol anesthesia. For all experimental conditions, the oral mucosa, entire gastrointestinal tract, spleen, liver, trachea, lungs, and neck lymph nodes were removed. For PET/CT experiments, tissues were cut into 1-cm^2 pieces and frozen in optimal cutting temperature (OCT) media (Thermo Fisher Scientific). Once frozen tissue was no longer radioactive, it was shipped on dry ice to the Hope Lab at Northwestern University. For experiments examining LICh transduced and SHIV-1157ipd3N4 infected cells, samples were stored in RPMI after necropsy, and shipped on ice overnight to Northwestern University.

NHP studies: imaging (PET, CT, and IVIS)

Animals were sedated with intramuscularly with 10mg/kg Telazol/ketamine (Zoeis, Parsippany-Troy Hills, New Jersey) and 1-3% isoflurane in 100% oxygen for the following scans. The animal's body was immobilized in dorsal recumbency in a vacuum-sealed veterinary positioner, and body temperature maintained with a warm air blanket (3M Bair hugger Model 505 warming unit, Saint Paul, Minnesota) and water-circulating heating pads. In addition, respiration, movement, and mucosal coloration (PET Scanner) were visually assessed. PET/CT scans were acquired using a Philips Gemini TF64 PET/CT scanner. The final CT image was compiled from 250 to 300 slices, depending on animal size. PET-CT combined images were analyzed using MIM software. Standard uptake values were measured using the volume regions of interest (ROI) tool and compared and normalized across animals. All scans lasted 20 minutes. Initial PET scans were obtained immediately following oral viral challenge. Second scans were

performed one hour after oral challenge. PET scans also occurred at two and four hours for final *in vivo* tracking of radiolabeled virus. CT scans were performed immediately following the last PET scan. After sacrifice, PET images of whole tissues were taken. After tissue processing, each block was scanned and compared to a standard control for PET intensity.

Tissues were soaked in 100mM d-Luciferin (Biosynth) for a minimum of 10 minutes and placed in *In Vivo* Imaging System (IVIS) machine to examine luciferase activity (Figure 1B). Tissues positive for luciferase were cut into 1x1 mm^2 pieces and frozen in optimal cutting temperature (OCT) media for PCR and microscopy. For experiments with PA-GFP-BaL, four animals received 0.5mL ^{64}Cu-PA-GFP-BaL and unlabeled 1mL of PA-GFP-BaL in Pedialyte. Animals were humanely sacrificed with an overdose of a solution containing pentobarbital (100mg/kg) while under isoflurane anesthesia. For all experimental conditions, the oral mucosa and GI tract were removed and separated by individual tissues, mesenteric lymph nodes were separated from the colon and stored as individual lymph nodes. All tissues were frozen in optimal cutting temperature media (OCT) for microscopy.

Nested PCR

Genomic DNA for nested PCR was isolated from frozen tissue sections embedded in OCT using the Qiagen DNeasy Blood and Tissue Kit as per the manufacturer's instructions. The initial nested PCR reactions were performed with 250ng of DNA per reaction and DreamTaq (Thermo Scientific). The second round of PCR was performed using 2ul of the first-round reaction products. For detection of LICh transduction, PCR was performed to identify mCherry DNA using the following primers: outside forward 5'-ACATGTGTTTAGTCGAGG-3', outside reverse 5'-CAGTCAATCTTTCACAAATTTTGTAATCC -3', inside forward 5'-CCGACTACTTGAAGCTGTCCTT-3', and inside reverse 5'-

GTCTTGACCTCAGCGTCGTAGT-3'. For detection of SHIV-1157ipd3N4 infection, PCR was performed to identify gag DNA using the following primers: outside forward 5'-ATTAGCAGAAAGCCTGTTGGAG-3', outside reverse 5'-AGAGTGTCCTTCTTTCCCACAA-3', inside forward 5'-CATTCACGCAGAAGAGAAAGTG-3', inside reverse 5'-GGTATGGGGTTCTGTTGTCTGT-3'. Each DNA sample was tested in 12 replicates. Sequences were confirmed by extracting DNA bands using Qaigen QIAquick Gel Extraction Kit and analysis with the second-round primers.

Fluorescent microscopy and image analysis

For all imaging, twelve-to-fifteen-micron tissue sections were cut and fixed with 3.7% formaldehyde in PIPES buffer for 10 minutes at room temperature. To study distributions and localization of PA-GFP-BaL, nuclei were stained with Hoechst (1:25,000, ThermoFisher Scientific). Coverslips were mounted with DakoCytomation mounting medium (Burlington, Ontario, Canada) and sealed with nail polish. Twenty to twenty-two Z-stack images at 0.5-μm steps were obtained by deconvolution microscopy on a DeltaVision inverted microscope (GE, Boston, Massachusetts) at 100x. The 20-22 images were taken in an unbiased manner by following the linear path of the luminal surface of the mucosa with the distance between each image dictated by bleaching caused by photoactivation. Images were analyzed with softWoRx software (Applied Precision, Issaquah, Washington). Number of total virions and penetrating virions were counted. Virions were defined by existing in more than three Z planes and the post-activation signal had to be at least three times higher than the pre-activation signal. Penetrating virions were defined by being at least 1μm deep into the epithelium; all penetration depths were measured in microns.

Tissue sections used to investigate infected cells were then washed in PBS and tissue sections were blocked in donkey serum (10% normal donkey serum, 0.1% Triton-X-100, 0.01% NaN_3) for 30 minutes at room temperature; blocking solution was used for staining buffer throughout experiment. For mCherry detection, tissue sections were stained with primary antibodies for CD3 (one drop of the prediluted antibody per 200µl staining buffer, clone SP7, Abcam) and HIV envelope (1:300 AG3, AIDS Reagent Repository) for two hours at room temperature. Slides were washed with PBS and then stained with secondary antibodies donkey anti-rabbit-AF488 and donkey anti-mouse-AF647 (1:1000, Jackson ImmunoResearch, West Grove, Pennsylvania) for one hour at room temperature. Nuclei were stained with Hoechst (1:25,000) for 10 minutes at room temperature. Adjacent tissue sections were stained with a primary rabbit anti-firefly luciferase (1:200, Abcam) for two hours at room temperature. Slides were washed with PBS and then stained with secondary antibodies donkey anti-rabbit-AF488 (1:1000). Nuclei were stained for with Hoechst (1:25000). Coverslips were mounted with DakoCytomation mounting medium and sealed with nail polish. Images were taken in 3x5 Z-stack panels at 0.5µm steps for 30 steps by deconvolution microscopy on a DeltaVision inverted microscope (GE) at 60x. Images were analyzed with softWoRx software (Applied Precision, Issaquah, Washington). Upon finding cells that appeared to be mCherry+, location of the cells was recorded, and sections were marked. Slides were then taken to an A1R-Spectral confocal microscope (Nikon, Tokyo, Japan) to analyze the emission spectra of the previously found cells compared to the known emission spectra of mCherry at 610nm. Images were analyzed with NIS Elements-C software (Nikon).

To phenotype of SHIV-1157ipd3N4 infected cells, slides were stained with primary antibodies for CD3 (one drop of the prediluted antibody per 200µl staining buffer, clone SP7,

Abcam) and HIV envelope (1:300 AG3, AIDS Reagent Repository) for two hours at room temperature. Slides were washed with PBS and then stained with secondary antibodies donkey anti-rabbit-AF488 and donkey anti-mouse-AF594 (1:1000, Jackson ImmunoResearch) for one hour at room temperature. Tissue sections were then washed and stained with an AF647-directly conjugated antibody towards CCR6 (1:200, clone G034E3, BioLegend) at 37^{o}C for one hour. Nuclei were stained for with Hoechst (1:25000). Coverslips were mounted with DakoCytomation mounting medium and sealed with nail polish. Image panels containing 30 sections in the Z plane at 0.5um steps were taken and deconvoluted with softWoRx software on a DeltaVision inverted microscope. Five 40x images were taken for each sample. Each image consisted of a stitched panel of three 40x images by 5 40x images to include the epithelium. Infected cells were counted, cell phenotypes were identified (T cells – $CD3^{+}$, Th17 cells – $CD3^{+}$ $CCR6^{+}$, immature dendritic cells – $CD3^{-}$, $CCR6^{+}$, and other – $CD3^{-}$, $CCR6^{-}$), and cell subsets were recorded as parts of a whole (100%).

Statistical Analysis

All statistical analyses were performed using R version 4.0.2. To perform group comparisons per necropsy time, different mixed-effects models were fitted separately for the 2- and 4-hour necropsy animals. For each dataset, we used the best fitting model depending on the nature of the data analyzed. We always included animal as a random effect in the models. Virion counts per necropsy time were modeled using a negative binomial generalized mixed model to test for differences between anatomical locations, controlling for the number of images taken per animal and tissue. For this dataset we also tested zero-inflated negative binomial models due to the high number of zeros observed in some anatomical regions, but these models did not significantly improve the performance of the negative binomial model. To test for differences in number of

622 penetrating virions present in the different anatomical locations per necropsy time, we
623 transformed the penetrating depth data into a binary categorical variable by considering
624 penetrating virions as those deeper than one micron from the epithelial surface data, while
625 defining the rest as non-penetrating virions. We subsequently fitted a binomial generalized linear
626 mixed-effects model including the anatomical location as the predictor variable, controlling for
627 the number of images taken per tissue and animal. Finally, we tested for differences in
628 penetrating depth among virions considered as penetrating by the previous definition between the
629 different anatomical locations. We used a linear mixed effects model, also controlling for
630 number of images. We performed all possible contrasts within each of the models, adjusting the
631 false discovery rate for multiple comparisons using Benjamini-Hochberg Procedure. A false
632 discovery rate (FDR) significance cut-off was set at FDR<0.05 for every comparison.

633 **Acknowledgements:** Thanks to the research and animal care teams at Texas Biomed and NIRC.
634 Thank you to Danijela Maric and Katarina Kotnik Halavaty for instruction on experimental
635 techniques.

636 **References**

637 1. Abel K. The rhesus macaque pediatric SIV infection model - a valuable tool in
638 understanding infant HIV-1 pathogenesis and for designing pediatric HIV-1 prevention strategies.
639 Current HIV research. 2009;7(1):2-11.
640 2. Iliff PJ, Piwoz EG, Tavengwa NV, Zunguza CD, Marinda ET, Nathoo KJ, et al. Early
641 exclusive breastfeeding reduces the risk of postnatal HIV-1 transmission and increases HIV-free
642 survival. AIDS (London, England). 2005;19(7):699-708.

643 3. Kuhn L, Sinkala M, Kankasa C, Semrau K, Kasonde P, Scott N, et al. High uptake of
644 exclusive breastfeeding and reduced early post-natal HIV transmission. PloS one.
645 2007;2(12):e1363.
646 4. Overbaugh J. Mother-infant HIV transmission: do maternal HIV-specific antibodies
647 protect the infant? PLoS pathogens. 2014;10(8):e1004283.
648 5. Gaur AH, Dominguez KL, Kalish ML, Rivera-Hernandez D, Donohoe M, Brooks JT, et
649 al. Practice of feeding premasticated food to infants: a potential risk factor for HIV transmission.
650 Pediatrics. 2009;124(2):658-66.
651 6. Ivy W, 3rd, Dominguez KL, Rakhmanina NY, Iuliano AD, Danner SP, Borkowf CB, et al.
652 Premastication as a route of pediatric HIV transmission: case-control and cross-sectional
653 investigations. Journal of acquired immune deficiency syndromes (1999). 2012;59(2):207-12.
654 7. Van Rompay KK, Greenier JL, Cole KS, Earl P, Moss B, Steckbeck JD, et al.
655 Immunization of newborn rhesus macaques with simian immunodeficiency virus (SIV) vaccines
656 prolongs survival after oral challenge with virulent SIVmac251. Journal of virology.
657 2003;77(1):179-90.
658 8. Stahl-Hennig C, Steinman RM, Tenner-Racz K, Pope M, Stolte N, Matz-Rensing K, et al.
659 Rapid infection of oral mucosal-associated lymphoid tissue with simian immunodeficiency virus.
660 Science. 1999;285(5431):1261-5.
661 9. Milush JM, Stefano-Cole K, Schmidt K, Durudas A, Pandrea I, Sodora DL. Mucosal innate
662 immune response associated with a timely humoral immune response and slower disease
663 progression after oral transmission of simian immunodeficiency virus to rhesus macaques. Journal
664 of virology. 2007;81(12):6175-86.

10. Milush JM, Kosub D, Marthas M, Schmidt K, Scott F, Wozniakowski A, et al. Rapid dissemination of SIV following oral inoculation. AIDS (London, England). 2004;18(18):2371-80.

11. Amedee AM, Phillips B, Jensen K, Robichaux S, Lacour N, Burke M, et al. Early Sites of Virus Replication After Oral SIVmac251 Infection of Infant Macaques: Implications for Pathogenesis. AIDS research and human retroviruses. 2018;34(3):286-99.

12. Douek DC, Brenchley JM, Betts MR, Ambrozak DR, Hill BJ, Okamoto Y, et al. HIV preferentially infects HIV-specific CD4+ T cells. Nature. 2002;417(6884):95-8.

13. Kou J, Kuang YQ. Mutations in chemokine receptors and AIDS. Progress in molecular biology and translational science. 2019;161:113-24.

14. Wang X, Rasmussen T, Pahar B, Poonia B, Alvarez X, Lackner AA, et al. Massive infection and loss of CD4+ T cells occurs in the intestinal tract of neonatal rhesus macaques in acute SIV infection. Blood. 2007;109(3):1174-81.

15. Wang X, Xu H, Pahar B, Alvarez X, Green LC, Dufour J, et al. Simian immunodeficiency virus selectively infects proliferating CD4+ T cells in neonatal rhesus macaques. Blood. 2010;116(20):4168-74.

16. Jaspan HB, Lawn SD, Safrit JT, Bekker LG. The maturing immune system: implications for development and testing HIV-1 vaccines for children and adolescents. AIDS (London, England). 2006;20(4):483-94.

17. Simon AK, Hollander GA, McMichael A. Evolution of the immune system in humans from infancy to old age. Proc Biol Sci. 2015;282(1821):20143085.

18. Abel K, Pahar B, Van Rompay KK, Fritts L, Sin C, Schmidt K, et al. Rapid virus dissemination in infant macaques after oral simian immunodeficiency virus exposure in the presence of local innate immune responses. Journal of virology. 2006;80(13):6357-67.

688 19. Thome JJ, Bickham KL, Ohmura Y, Kubota M, Matsuoka N, Gordon C, et al. Early-life
689 compartmentalization of human T cell differentiation and regulatory function in mucosal and
690 lymphoid tissues. Nature medicine. 2016;22(1):72-7.
691 20. Rudd BD. Neonatal T Cells: A Reinterpretation. Annual review of immunology.
692 2020;38:229-47.
693 21. Bixler SL, Mattapallil JJ. Loss and dysregulation of Th17 cells during HIV infection.
694 Clinical & developmental immunology. 2013;2013:852418.
695 22. Stieh DJ, Matias E, Xu H, Fought AJ, Blanchard JL, Marx PA, et al. Th17 Cells Are
696 Preferentially Infected Very Early after Vaginal Transmission of SIV in Macaques. Cell host &
697 microbe. 2016;19(4):529-40.
698 23. Hartigan-O'Connor DJ, Abel K, McCune JM. Suppression of SIV-specific CD4+ T cells
699 by infant but not adult macaque regulatory T cells: implications for SIV disease progression. The
700 Journal of experimental medicine. 2007;204(11):2679-92.
701 24. D'Ettorre G, Borrazzo C, Pinacchio C, Santinelli L, Cavallari EN, Statzu M, et al. Increased
702 IL-17 and/or IFN-gamma producing T cell subsets in gut mucosa of long-term treated HIV-1-
703 infected women. AIDS (London, England). 2019.
704 25. Van Rompay KK, Abel K, Lawson JR, Singh RP, Schmidt KA, Evans T, et al. Attenuated
705 poxvirus-based simian immunodeficiency virus (SIV) vaccines given in infancy partially protect
706 infant and juvenile macaques against repeated oral challenge with virulent SIV. Journal of acquired
707 immune deficiency syndromes (1999). 2005;38(2):124-34.
708 26. Santangelo PJ, Rogers KA, Zurla C, Blanchard EL, Gumber S, Strait K, et al. Whole-body
709 immunoPET reveals active SIV dynamics in viremic and antiretroviral therapy-treated macaques.
710 Nat Methods. 2015;12(5):427-32.

711 27. Xie H, Wang ZJ, Bao A, Goins B, Phillips WT. In vivo PET imaging and biodistribution
712 of radiolabeled gold nanoshells in rats with tumor xenografts. Int J Pharm. 2010;395(1-2):324-30.
713 28. Carias AM, McCoombe S, McRaven M, Anderson M, Galloway N, Vandergrift N, et al.
714 Defining the interaction of HIV-1 with the mucosal barriers of the female reproductive tract.
715 Journal of virology. 2013;87(21):11388-400.
716 29. McDonald D, Vodicka MA, Lucero G, Svitkina TM, Borisy GG, Emerman M, et al.
717 Visualization of the intracellular behavior of HIV in living cells. The Journal of cell biology.
718 2002;159(3):441-52.
719 30. Taylor RA, Xiao S, Carias AM, McRaven MD, Thakkar DN, Araínga M, et al. PET/CT
720 targeted tissue sampling reveals virus specific dIgA can alter the distribution and localization of
721 HIV after rectal exposure. PLoS pathogens. 2021;17(6):e1009632.
722 31. Stieh DJ, Maric D, Kelley ZL, Anderson MR, Hattaway HZ, Beilfuss BA, et al. Vaginal
723 challenge with an SIV-based dual reporter system reveals that infection can occur throughout the
724 upper and lower female reproductive tract. PLoS pathogens. 2014;10(10):e1004440.
725 32. Song RJ, Chenine AL, Rasmussen RA, Ruprecht CR, Mirshahidi S, Grisson RD, et al.
726 Molecularly cloned SHIV-1157ipd3N4: a highly replication- competent, mucosally transmissible
727 R5 simian-human immunodeficiency virus encoding HIV clade C Env. Journal of virology.
728 2006;80(17):8729-38.
729 33. Tenner-Racz K, Stahl Hennig C, Uberla K, Stoiber H, Ignatius R, Heeney J, et al. Early
730 protection against pathogenic virus infection at a mucosal challenge site after vaccination with
731 attenuated simian immunodeficiency virus. Proceedings of the National Academy of Sciences of
732 the United States of America. 2004;101(9):3017-22.

733 34. Veazey RS, Lifson JD, Pandrea I, Purcell J, Piatak M, Jr., Lackner AA. Simian
734 immunodeficiency virus infection in neonatal macaques. Journal of virology. 2003;77(16):8783-
735 92.
736 35. Holl V, Xu K, Peressin M, Lederle A, Biedma ME, Delaporte M, et al. Stimulation of HIV-
737 1 replication in immature dendritic cells in contact with primary CD4 T or B lymphocytes. Journal
738 of virology. 2010;84(9):4172-82.
739 36. Hu J, Miller CJ, O'Doherty U, Marx PA, Pope M. The dendritic cell-T cell milieu of the
740 lymphoid tissue of the tonsil provides a locale in which SIV can reside and propagate at chronic
741 stages of infection. AIDS research and human retroviruses. 1999;15(14):1305-14.
742 37. Wiley RD, Gummuluru S. Immature dendritic cell-derived exosomes can mediate HIV-1
743 trans infection. Proceedings of the National Academy of Sciences of the United States of America.
744 2006;103(3):738-43.
745 38. Baba TW, Koch J, Mittler ES, Greene M, Wyand M, Penninck D, et al. Mucosal infection
746 of neonatal rhesus monkeys with cell-free SIV. AIDS research and human retroviruses.
747 1994;10(4):351-7.
748 39. Marthas ML, van Rompay KK, Otsyula M, Miller CJ, Canfield DR, Pedersen NC, et al.
749 Viral factors determine progression to AIDS in simian immunodeficiency virus-infected newborn
750 rhesus macaques. Journal of virology. 1995;69(7):4198-205.
751 40. Miclat NN, Hodgkinson R, Marx GF. Neonatal gastric pH. Anesth Analg. 1978;57(1):98-
752 101.
753 41. Dudley JP, Golovkina TV, Ross SR. Lessons Learned from Mouse Mammary Tumor Virus
754 in Animal Models. Ilar j. 2016;57(1):12-23.

755 42. Ross SR. Mouse mammary tumor virus molecular biology and oncogenesis. Viruses.
756 2010;2(9):2000-12.
757 43. Wood LF, Chahroudi A, Chen HL, Jaspan HB, Sodora DL. The oral mucosa immune
758 environment and oral transmission of HIV/SIV. Immunological reviews. 2013;254(1):34-53.
759 44. Durudas A, Chen HL, Gasper MA, Sundaravaradan V, Milush JM, Silvestri G, et al.
760 Differential innate immune responses to low or high dose oral SIV challenge in Rhesus macaques.
761 Current HIV research. 2011;9(5):276-88.
762 45. Van Rompay KK, Schmidt KA, Lawson JR, Singh R, Bischofberger N, Marthas ML.
763 Topical administration of low-dose tenofovir disoproxil fumarate to protect infant macaques
764 against multiple oral exposures of low doses of simian immunodeficiency virus. The Journal of
765 infectious diseases. 2002;186(10):1508-13.
766 46. Ndirangu J, Viljoen J, Bland RM, Danaviah S, Thorne C, Van de Perre P, et al. Cell-free
767 (RNA) and cell-associated (DNA) HIV-1 and postnatal transmission through breastfeeding. PloS
768 one. 2012;7(12):e51493.
769 47. Rousseau CM, Nduati RW, Richardson BA, Steele MS, John-Stewart GC, Mbori-Ngacha
770 DA, et al. Longitudinal analysis of human immunodeficiency virus type 1 RNA in breast milk and
771 of its relationship to infant infection and maternal disease. The Journal of infectious diseases.
772 2003;187(5):741-7.
773 48. Willumsen JF, Filteau SM, Coutsoudis A, Newell ML, Rollins NC, Coovadia HM, et al.
774 Breastmilk RNA viral load in HIV-infected South African women: effects of subclinical mastitis
775 and infant feeding. AIDS (London, England). 2003;17(3):407-14.
776 49. Patterson GH, Lippincott-Schwartz J. A photoactivatable GFP for selective photolabeling
777 of proteins and cells. Science. 2002;297(5588):1873-7.

778 50. Nègre D, Mangeot PE, Duisit G, Blanchard S, Vidalain PO, Leissner P, et al.
779 Characterization of novel safe lentiviral vectors derived from simian immunodeficiency virus
780 (SIVmac251) that efficiently transduce mature human dendritic cells. Gene Ther.
781 2000;7(19):1613-23.
782 51. Rabinovich BA, Ye Y, Etto T, Chen JQ, Levitsky HI, Overwijk WW, et al. Visualizing
783 fewer than 10 mouse T cells with an enhanced firefly luciferase in immunocompetent mouse
784 models of cancer. Proceedings of the National Academy of Sciences of the United States of
785 America. 2008;105(38):14342-6.

786 **Fig 1: PET imaging follows distribution of PA-BaL-^{64}Cu after oral viral challenge** Four
787 animals were orally challenged with PA-GFP-BaL-^{64}Cu. Two animals were sacrificed two hours
788 post challenge and another two four hours post challenge, and the oral cavity and entire GI tract
789 removed in one piece. The tissues were cut into pieces, frozen, cryosectioned, and prepared for
790 fluorescent microscopy. **A,B)** Representative PET images of neonates after oral viral challenge
791 with PA-GFP-BaL-^{64}Cu. Scale in Standard Uptake Value (SUV) **(A)** Whole body PET images at
792 two and four hours post-oral challenge. **B)** PET image overlayed on photograph of 25 individual
793 tissue blocks from oral mucosa and GI tract four hours post-challenge. **C)** Representative
794 fluorescent microscopy image showing individual HIV virions (red puncta indicated by white
795 arrows) penetrating the tongue of an animal that received PA-BaL-^{64}Cu at two hours post-
796 challenge. Green – pre-activation, Red – post-activation (virion), Blue – Hoechst
797

798 **Fig 2: HIV virions distribute throughout and penetrate the mucosal epithelium of the**
799 **entire GI tract four hours post-oral challenge** Whole GI tracts were excised and imaged by
800 PET at two- and four-hours following necropsy. PET images overlayed on photographs allow for

visualization of radioactivity throughout the GI tract at two hours **(A-B)** and four hours **(C-D)** post challenge. White dotted lines depict where the GI tracts were dichotomized into upper (esophagus and stomach) and lower (small and large intestines) regions. Quantification of virions and viral penetration in the oral cavity, upper GI tract, and lower GI tract mucosa two and four hours after oral viral challenge. **E)** Total number of virions counted in images. Means of the virion count per group shown on stacked bars in white numbers. **F)** Frequency of total virions counted. **G)** Quantification of the number of penetrating virions. Circle area represents the number of virions. **H)** Virion penetration depth in microns. Each virion depth was truncated to integer numbers for representation purposes. Circle area represents the number of virions with the same depth value. Blue: two hours, Red: four hours

Fig 3: Detection of LICh transduced cells after oral challenge Eight animals were orally challenged with LICh and SHIV-1157ipd3N4 and sacrificed at 96 hours. Tissues were dissected, analyzed by IVIS, frozen and tissue blocks with high luciferase activity were cryosectioned. Representative fluorescent microscopy images. **A)** Images of neonatal tissue showing luciferase activity on IVIS **B)** Image of LICh transduced cell (Cell 2) in the tongue of RM22. Cell 2 indicates a possible mCherry+ cell, Cell 1 indicates a neighboring cell with red background signal. Red – mCherry, green – CD3, Blue – Hoechst. 40x panel, scale bar is 30 μm **C)** Spectral imaging confirms mCherry signal in Cell 2 by comparison to known mCherry spectral emission. Green – Cell 1, Red – Cell 2, Blue – known mCherry emission **D)** Image of tongue showing no luciferase staining or mCherry label, suggesting LICh may not be sufficient in determining first cell infected in neonate oral challenge model. Red – mCherry, green – luciferase, Blue – Hoechst. 40x panel, scale bar is 30μm

Fig 4: The majority of SHIV-1157ipd3N4 infected cells are found in the small intestine 96 hours after oral challenge. Fluorescent microscopy and quantification of SHIV-1157ipd3N4 infected cells from eight animals that were sacrificed at 96 hours after dual viral oral challenge. Tissues were dissected, analyzed by IVIS, frozen, and tissue blocks with high luciferase activity were cryosectioned. Slides were stained for CD3, CCR6, AG3, and Hoechst. Representative fluorescent microscopy images. **A-B)** Cryosections of the small intestine showing SHIV-1157ipd3N4 infected cells **A)** 40X panels, scale bars 60 microns **B)** 100x panels, scale bars 20 microns **C)** Quantification of total number of SHIV-1157ipd3N4 infected cells by tissue type. Each dot represents the total number of cells found in five 40x panels in one individual animal

Fig 5: The majority of SHIV-1157ipd3N4 infected cells are T cells at 96 hours after oral challenge Quantification of SHIV-1157ipd3N4 infected cells found in the oral cavity and GI tract of animals examined in Figures 4-5. Graphs depict the percentage of infected cell types identified by fluorescent microscopy as parts of a whole. Total cell counts were taken in five 40x panels in every animal. **A)** Total number of infected cells in all eight neonatal RMs in tongue, tonsil, esophagus, stomach, small intestine, and large intestine. **B)** Total number of infected cell phenotypes in all eight RMs in the stomach, small intestine, and large intestine. Infected cell types were categorized as five cell types: T cells (CD3+), TH17 T cells (CD3+, CCR6+), other T cells (CD3+, CCR6-), Immature DCs (CD3-, CCR6+), Other (CD3-, CCR6-).

S1 Fig: Phenotype of SHIV-1157ipd3N4 infected cells in neonatal RM after oral viral exposure Quantification of SHIV-1157ipd3N4 infected cells found in the GI tract of each animal

847 examined in Figures 4-5. Graphs depict the percentage of infected cell types as parts of a whole
848 in each individual animal identified by fluorescent microscopy. Infected cell types were
849 categorized as five cell types: T cells (CD3+), TH17 T cells (CD3+, CCR6+), other T cells
850 (CD3+, CCR6-), Immature DCs (CD3-, CCR6+), Other (CD3-, CCR6-). Total cell counts were
851 taken in five 40x panels in every animal.
852
853 **Table 1: Distribution of LICh transduction and SHIV-1157ipd3N4 DNA throughout the GI**
854 **tract after oral challenge** LICh viral vector mainly found in the tongue after oral challenge.
855 SHIV-1157ipd3N4 viral dissemination found throughout the GI tract after oral challenge. +
856 indicates mCherry DNA found; # indicates gag DNA found
857 **Table 2: Localization of LICh transduced cells at 96 hours post oral challenge by**
858 **microscopy** LICh transduced cells found in the tongue, trachea, and stomach 96 hours after oral
859 challenge by microscopy. Cells were validated by spectral imaging. + indicates mCherry DNA
860 found
861 **Table 3: Localization of SHIV-1157ipd3N4 infected cells 96 hours after oral challenge by**
862 **microscopy** SHIV-1157ipd3N4 viral dissemination found throughout the GI tract after oral
863 challenge. + indicates AG3+ cells found by microscopy, NA indicates mesenteric lymph nodes
864 were not collected from this animal
865 **S1 Table: Identification of neonatal rhesus macaques used in LICh and SHIV-1157ipd3N4**
866 **studies** *Day of harvest, date of harvest, initials of scientists who grew virus listed

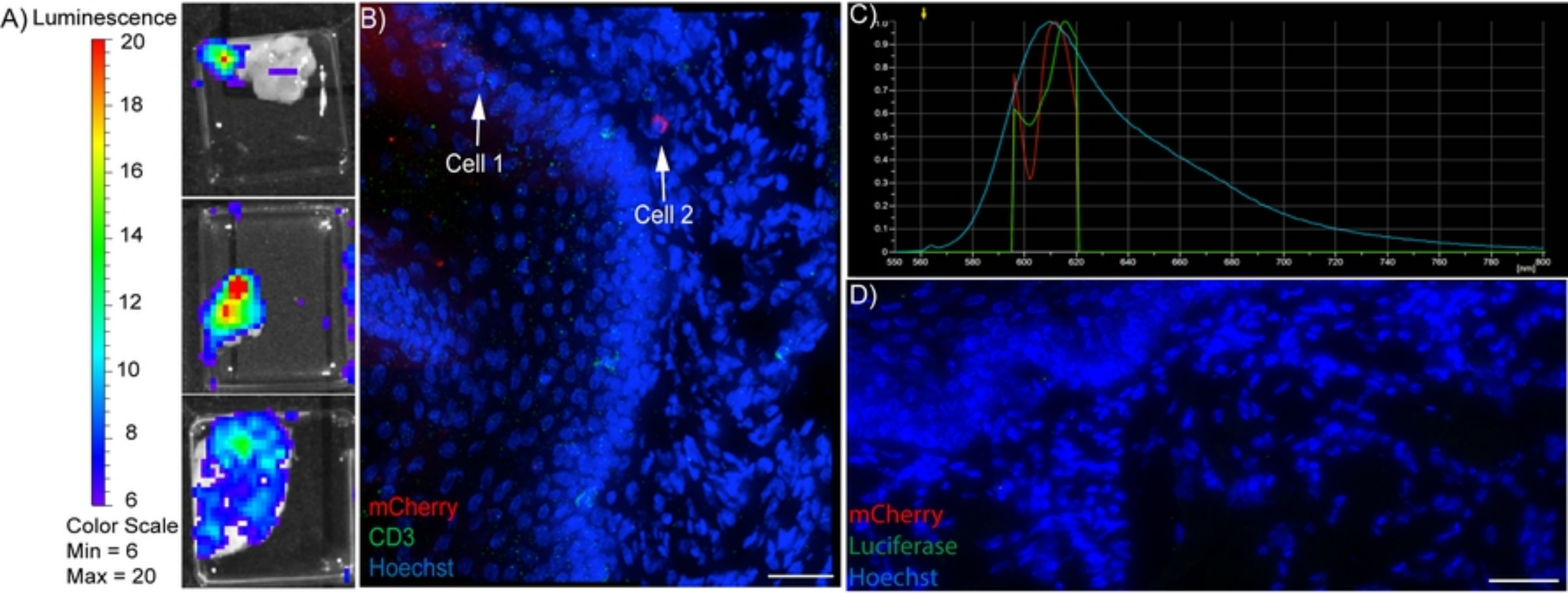
A) Luminescence
20
18
16
14
12
10
8
6
Color Scale
Min = 6
Max = 20
B)
Cell 1
Cell 2
mCherry
CD3
Hoechst
C)
D)
mCherry
Luciferase
Hoechst

Fig3

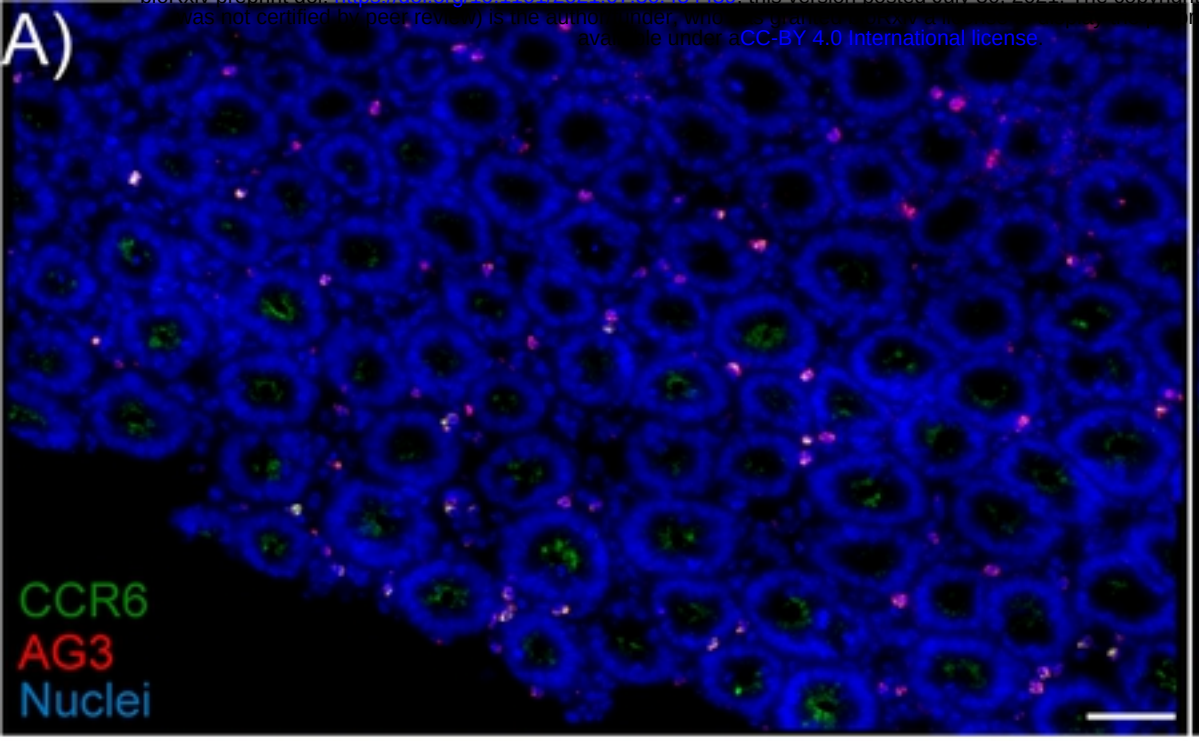

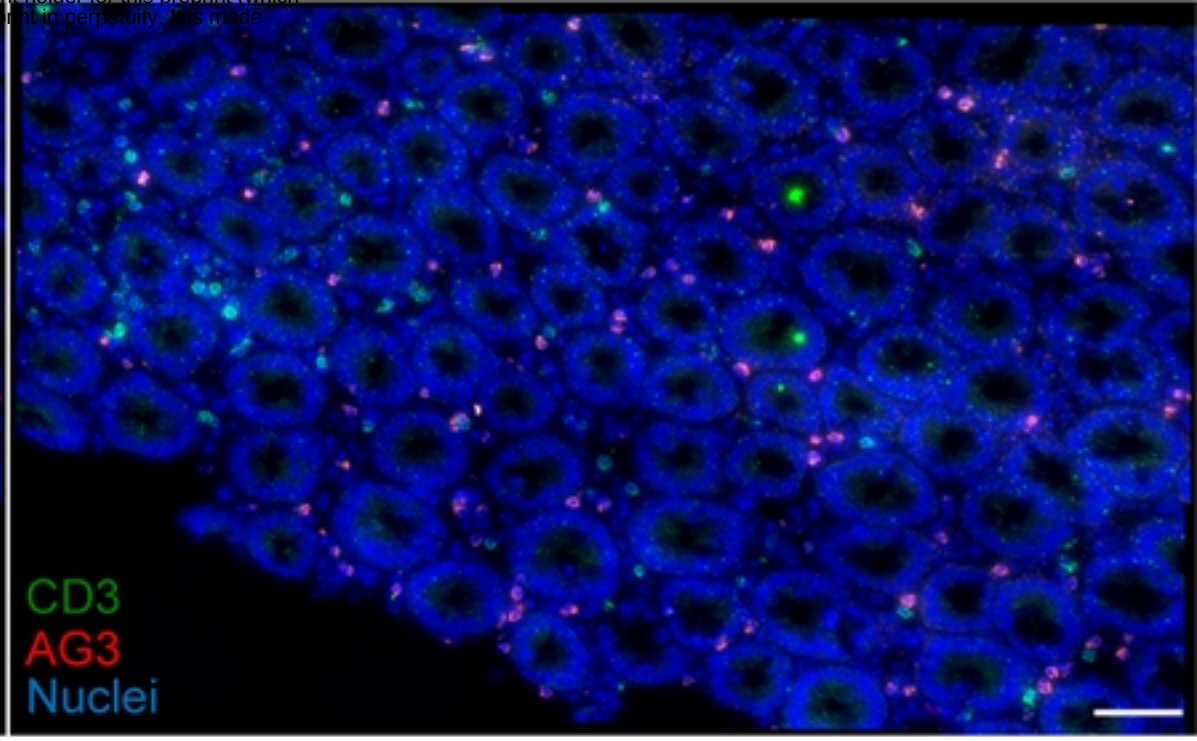

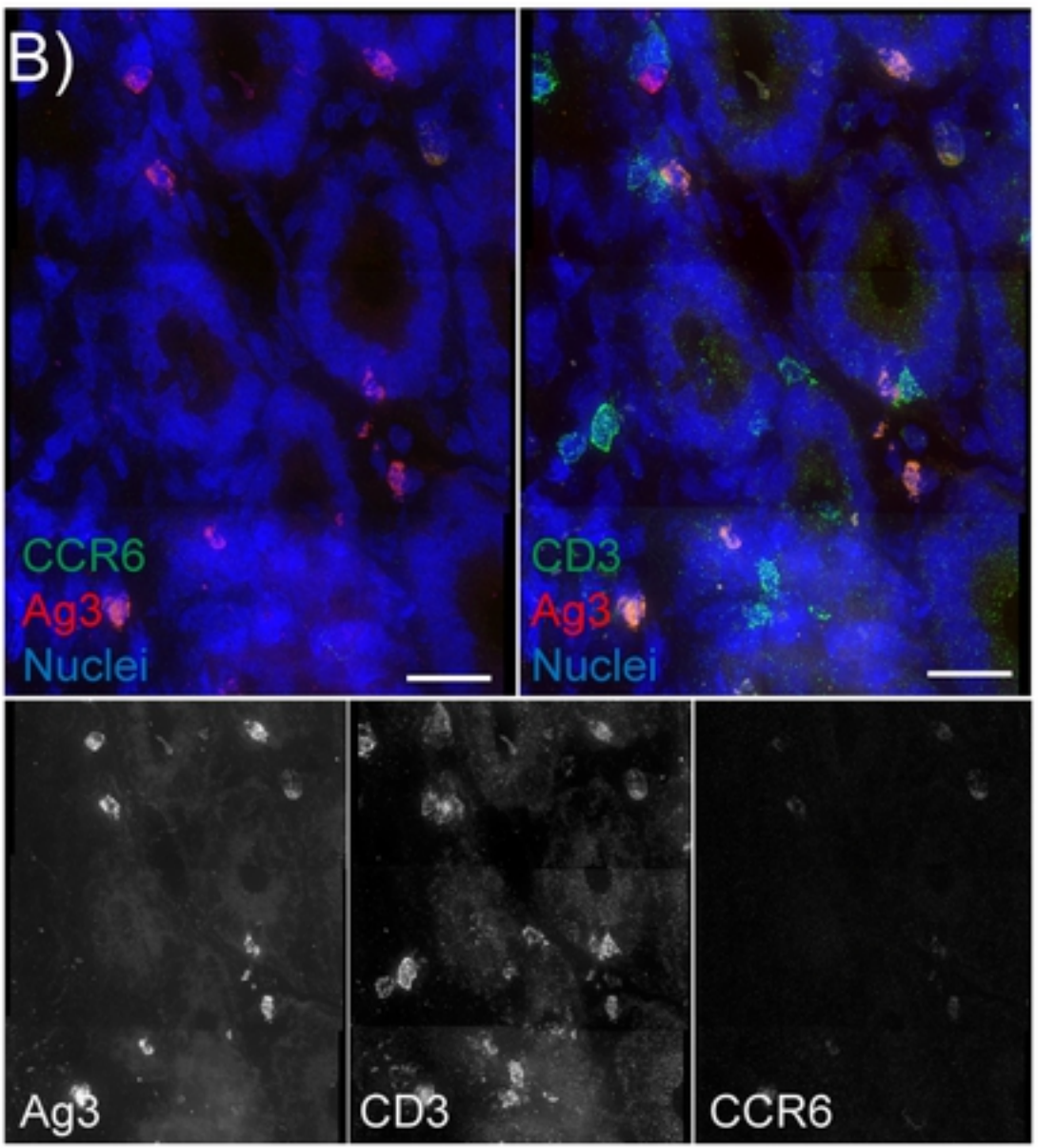

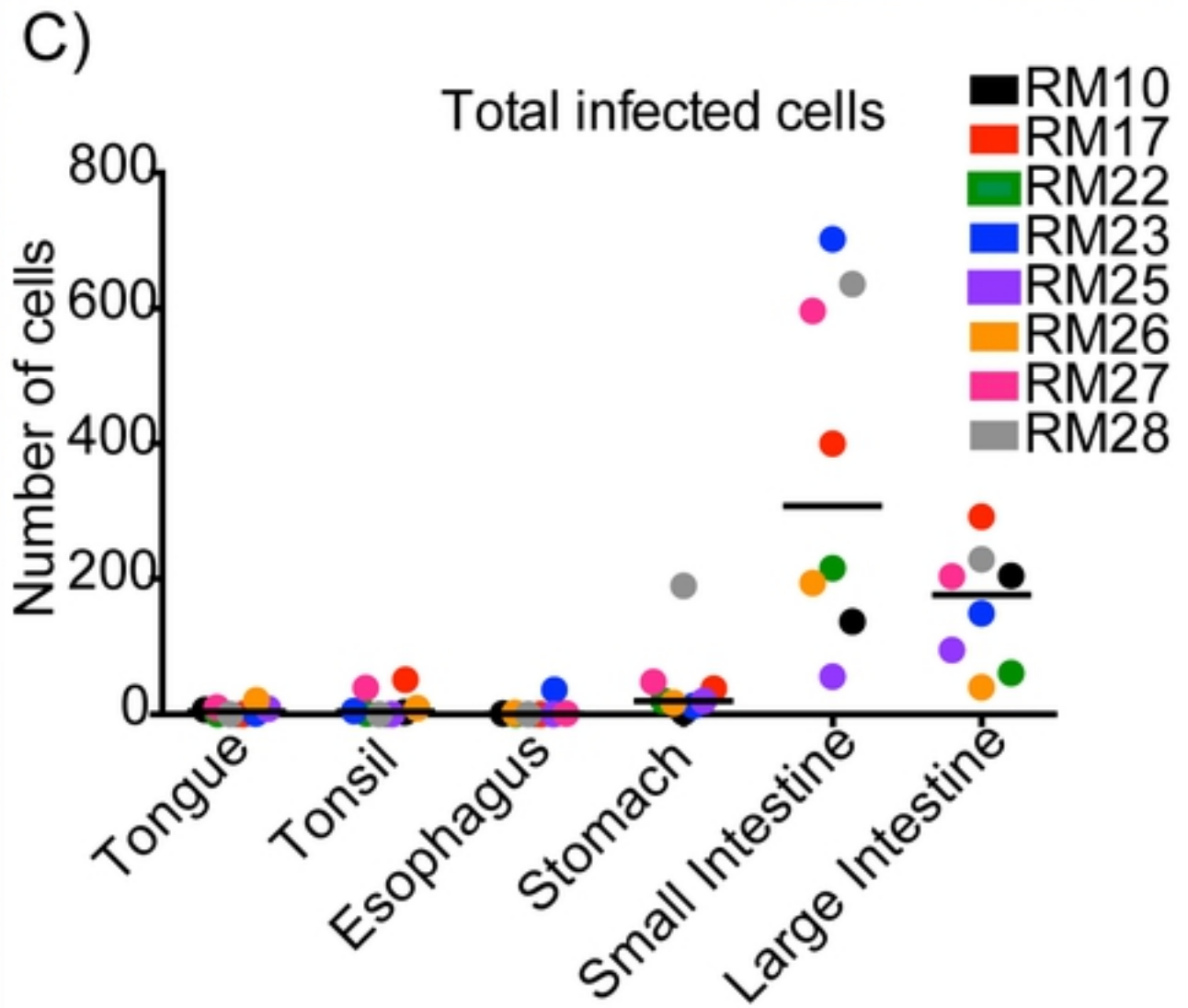

Fig4

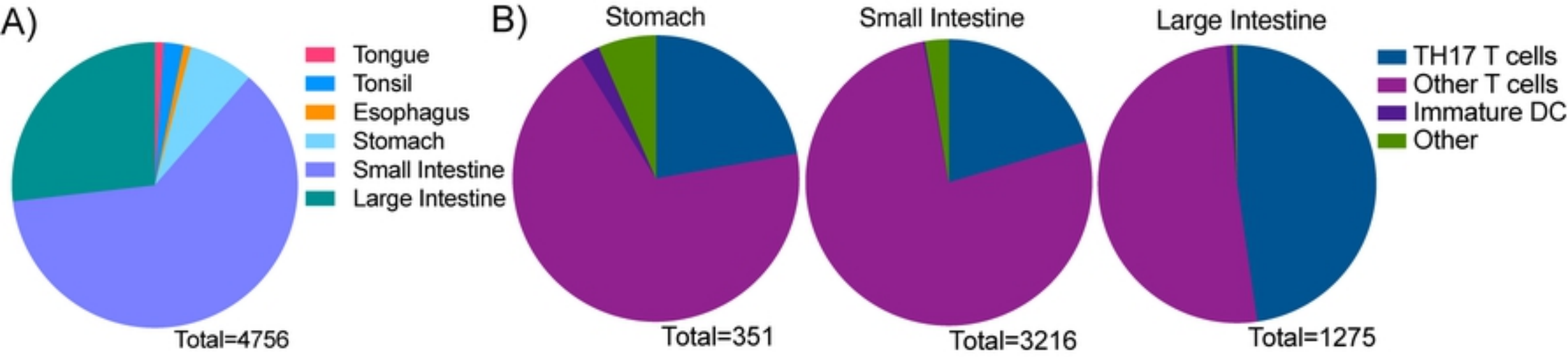
A)
Tongue
Tonsil
Esophagus
Stomach
Small Intestine
Large Intestine
Total=4756
B)
Stomach
Small Intestine
Large Intestine
TH17 T cells
Other T cells
Immature DC
Other
Total=351
Total=3216
Total=1275

Fig5

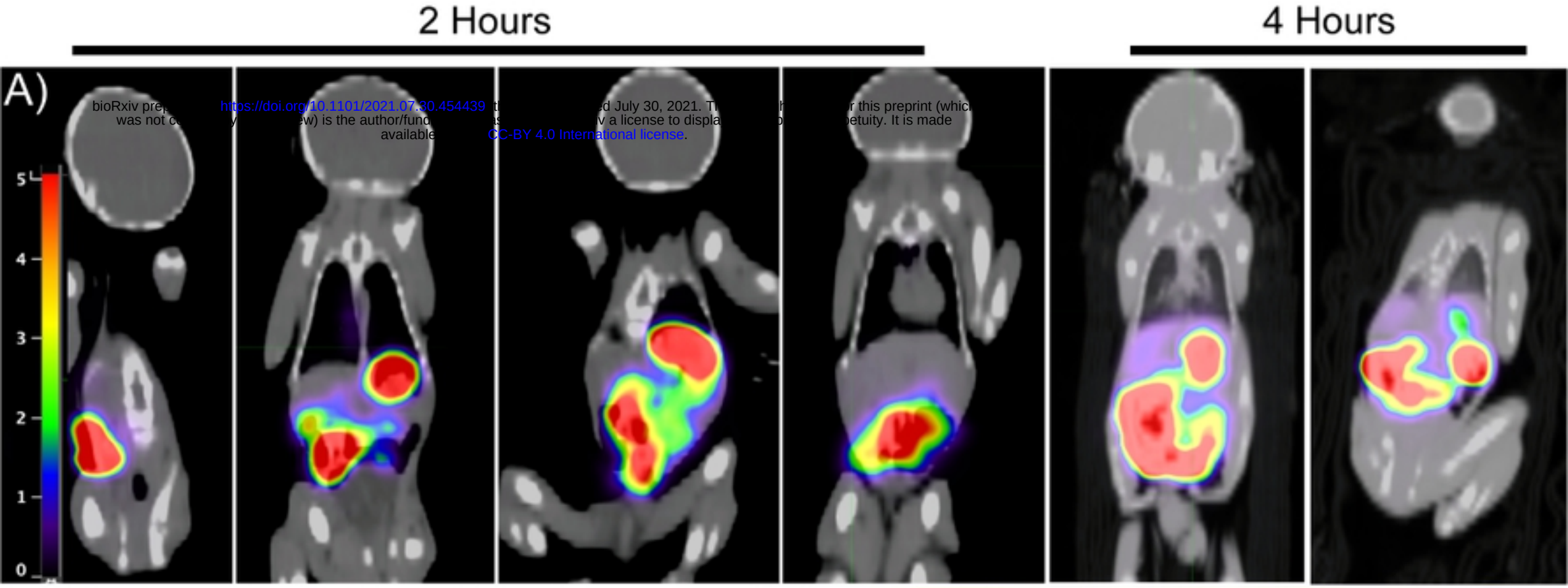

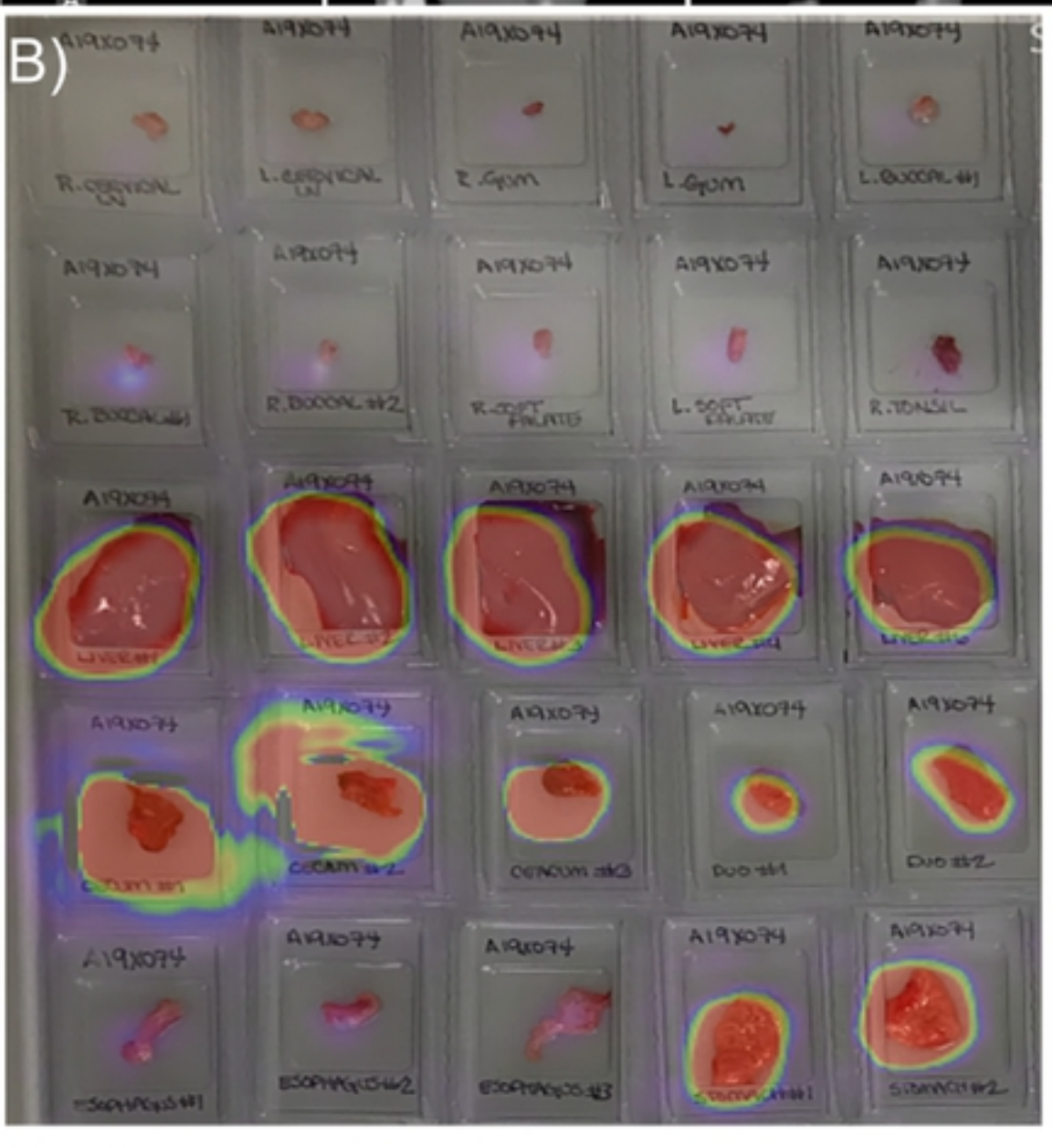

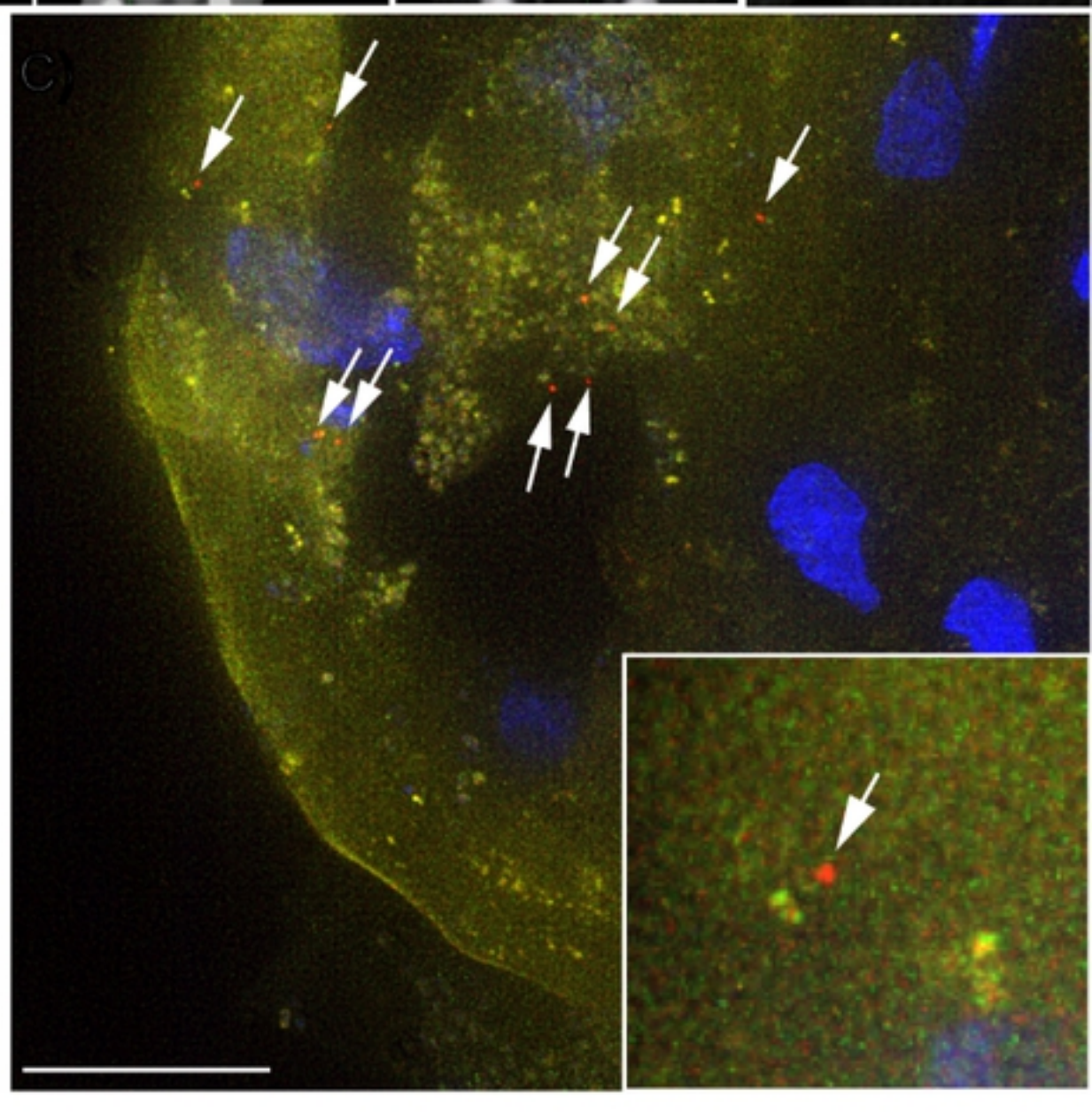

Fig1

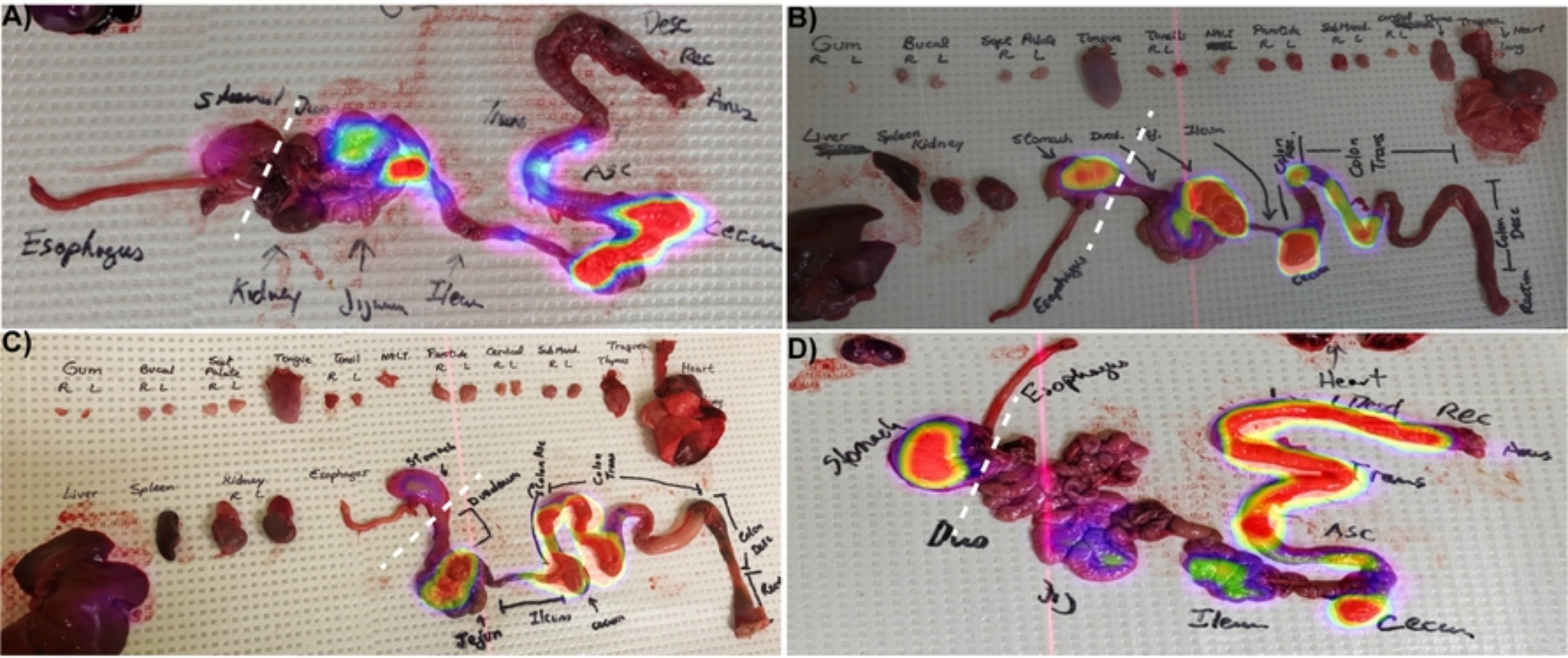
A)
Esophagus
Kidney
Jejunum
Ileum
Cecum
Asc
Trans
Desc
Rec
Anus
B)
Gum
Buccal
Soft Palate
Tongue
Tonsil
NALT
Parotid
Sub.Mand.
Thymus
Heart
Liver
Spleen
Kidney
Stomach
Duod.
Jej.
Ileum
Colon Asc
Colon Trans
Colon Desc
Cecum
Esophagus
Rectum
C)
Gum
Buccal
Soft Palate
Tongue
Tonsil
NALT
Parotid
Cervical
Sub.Mand.
Tongue Thymus
Heart
Liver
Spleen
Kidney
Esophagus
Stomach
Duodenum
Colon Asc
Colon Trans
Colon Desc
Rectum
Jejun
Ileum
Cecum
D)
Esophagus
Heart
Stomach
Duod
Rec
Anus
Trans
Asc
Duo
Jej
Ileum
Cecum

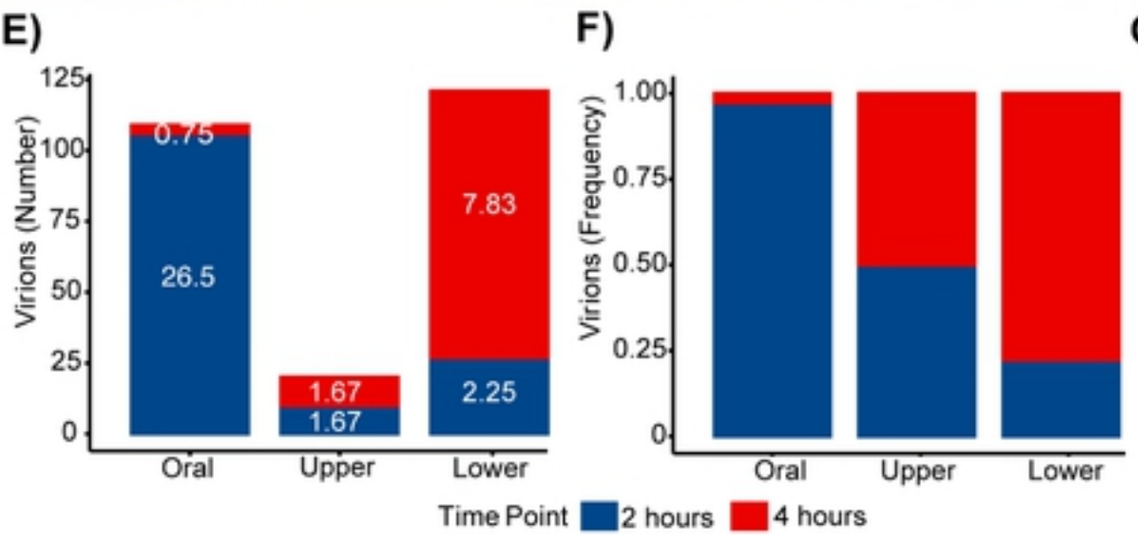
E)
Virions (Number)
125
100
75
50
25
0
0.75
26.5
1.67
1.67
7.83
2.25
Oral
Upper
Lower
F)
Virions (Frequency)
1.00
0.75
0.50
0.25
0
Oral
Upper
Lower
Time Point
2 hours
4 hours

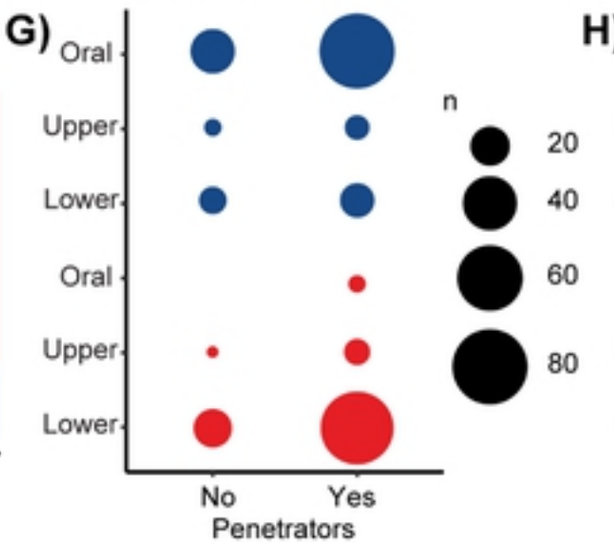
G)
Oral
Upper
Lower
Oral
Upper
Lower
n
20
40
60
80
No
Yes
Penetrators

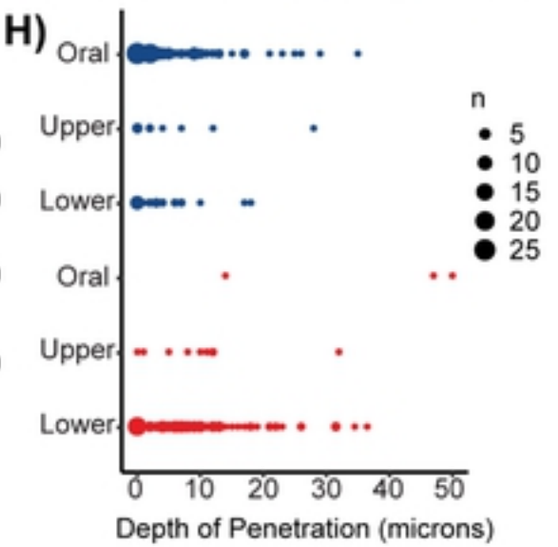
H)
Oral
Upper
Lower
Oral
Upper
Lower
n
5
10
15
20
25
0
10
20
30
40
50
Depth of Penetration (microns)

Fig2